INFORMATION BASED SMART RF ENERGY HARVESTING IN WIRELESS SENSOR NETWORKS

by

Asheesh Tripathi

A thesis submitted to the faculty of
The University of North Carolina at Charlotte
in partial fulfillment of the requirements
for the degree of Master of Science in
Electrical Engineering

Charlotte

2020

Approved by:

____

Dr. Asis Nasipuri

____

Dr. Ahmed Arafa

____

Dr. Thomas P. Weldon

ABSTRACT

ASHEESH TRIPATHI. Information based smart RF energy harvesting in wireless sensor networks. (Under the direction of DR. ASIS NASIPURI)

A major constraint for long term sustainability of wireless sensor networks (WSN) and the Internet of Things (IoT) is the limitation of their energy resources. Most wireless sensors are low energy consuming devices which are, in general, designed to transmit sporadically, and various energy saving techniques have been proposed to reduce the power consumption. However, battery replacement in sensor nodes can be a prohibitively expensive exercise because of their abundance. Dedicated RF energy harvesting (R-EH) has emerged as a promising technique to improve the lifespan, reliability, and capacity of WSN and IoT networks. This work evaluates the potential benefit of using a combination of an omnidirectional RF energy transmitter for getting periodic information updates, and then beam steering, by physically rotating a directional RF energy transmitter, to achieve higher sampling rates from the areas of need. An information based scheme for steering directional RF energy transmitter is presented that is based on the number of alarms (indication of abnormal events) received from the network. An energy harvesting development kit for wireless sensor network manufactured by Powercast Corporation is used for developing the proof of concept. This work is supported by extensive MATLAB simulations to analyze the proposed scheme performance in different network scenario. The simulation results show that the proposed maximum alarm based directional transmitter rotation scheme performs significantly better than the sequential transmitter rotation in terms of total abnormal events detected and alarms received per abnormal event occurred.

ACKNOWLEDGEMENTS

First of all, I would like to express my sincere gratitude to Dr. Asis Nasipuri for his invaluable guidance, motivation and support. His insight and expertise in this field has been inspiring and gave me a great learning experience. He has been patient and supportive all throughout the research and working under his supervision has indeed been a privilege.

I would like to extend my special thanks to my committee members Dr. Ahmed Arafa and Dr. Thomas P. Weldon for their guidance and support. Also, I would like to thank Mr. Eddie Hill for his assistance and help in lab supplies and Mr. Shobhit Aggarwal for all the help during experimental set up phase.

I would like to dedicate my thesis to my parents Mr. Mahesh Mani Tripathi, Mrs. Neelam Tripathi and, my sisters and brothers-in-law. I would like to specially mention my Fiancee Priyanka for her emotional support.

Last but never the least, I would like to thank all my friends and relatives who always encouraged me to move ahead and believed in me which was a boost to me while I was doing my research.

TABLE OF CONTENTS

LIST OF TABLES

LIST OF FIGURES

LIST OF ABBREVIATIONS

DC	An acronym for Direct Current.
ECE	An acronym for Electrical and Computer Engineering.
IEEE	An acronym for Institute of Electrical and Electronics Engineers.
IoT	An acronym for Internet of Things.
mF	An acronym for milli Farad.
ms	An acronym for milli Seconds.
R-EH	An acronym for RF Energy Harvesting .
RF	An acronym for Radio Frequency.
Tx	An acronym for Transmitter.
Vcap	An acronym for Voltage across Capacitor.
Vout	An acronym for Output Voltage.
WSN	An acronym for Wireless Sensor Network.

CHAPTER 1: INTRODUCTION

In recent years, WSN-based IoT has emerged as a promising technology with applications in many domains like smart city, home automation, health-care systems, and smart grid and transportation [2]. Wireless sensors are widely used to monitor physical or environmental conditions such as temperature, pollutants, pressure, motion, vibration, or sound at remote locations [3]. A WSN generally consists of a large number of sensor nodes with multimodal sensing as well as computation and wireless communication capabilities. Figure 1.1 demonstrates the functional subsystems of a wireless sensor node, which typically comprises: (i) a sensing subsystem (ii) a processing subsystem to locally process data, (iii) a wireless communication subsystem for transmitting data, and (iv) a power source (a battery with a limited energy budget or a energy harvesting system) to power the other subsystems.

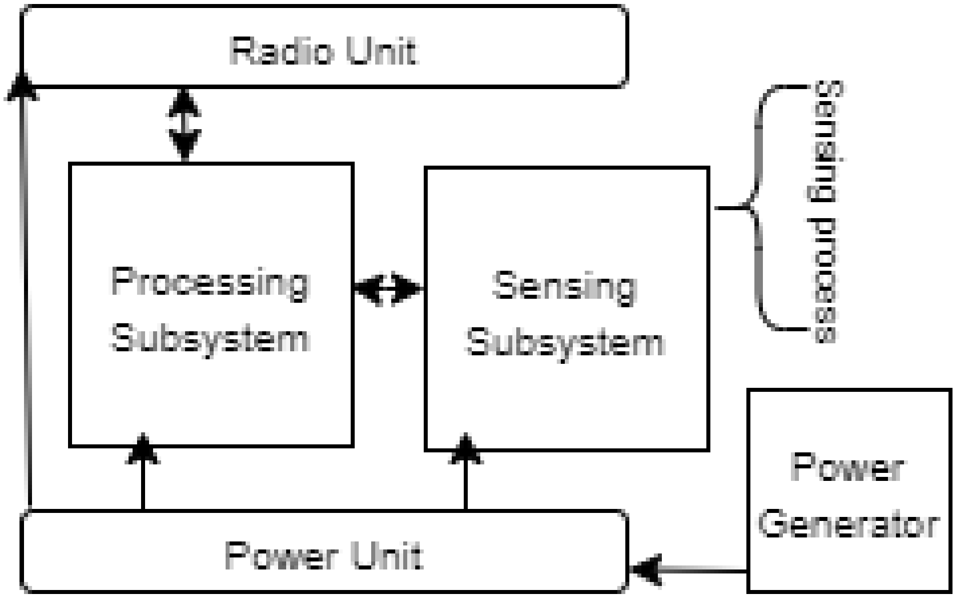

Figure 1.1: Functional subsystems of a wireless sensor node.

A key challenge in these networks is the limitation of energy supply since batteries need frequent replacement and involves human intervention, time, and cost. Furthermore, it becomes very difficult to replace the batteries due to the deployment of the nodes in hostile terrain or because of the large number of nodes deployed. These requirements highlight the need for different energy minimizing techniques or providing energy harvesting mechanisms for the sensor nodes[4]. Over the years, there has been a lot of focus on designing energy-efficient techniques and communication protocols to minimize the energy consumption of sensor nodes [5]. But, even though energy-efficient sensing and communication protocols can extend the battery life of the sensor nodes, the sensor node cannot operate once the limited battery energy is exhausted. A more promising approach is to harvest energy from the environment to keep the sensor nodes operational for an extended period of time.

Environmental energy harvesting techniques enable wireless sensor nodes to harvest energy from various energy sources such as solar power, wind, mechanical vibrations, electromagnetic fields, etc [6]. Figure 1.2 illustrates commonly used sources for energy harvesting. Table 1.1 illustrates the characteristics of a few ambient energy sources in terms of duration of energy availability, amount of energy available and the set up required to harvest energy from corresponding energy source. The random availability of ambient energy sources coupled with the limitations of supply and storage makes it difficult to operate wireless sensor nodes continuously for extended periods [7]. Also, for some applications, there may be a need to supply on-demand energy to a specific set of sensor nodes that have important information to transmit.

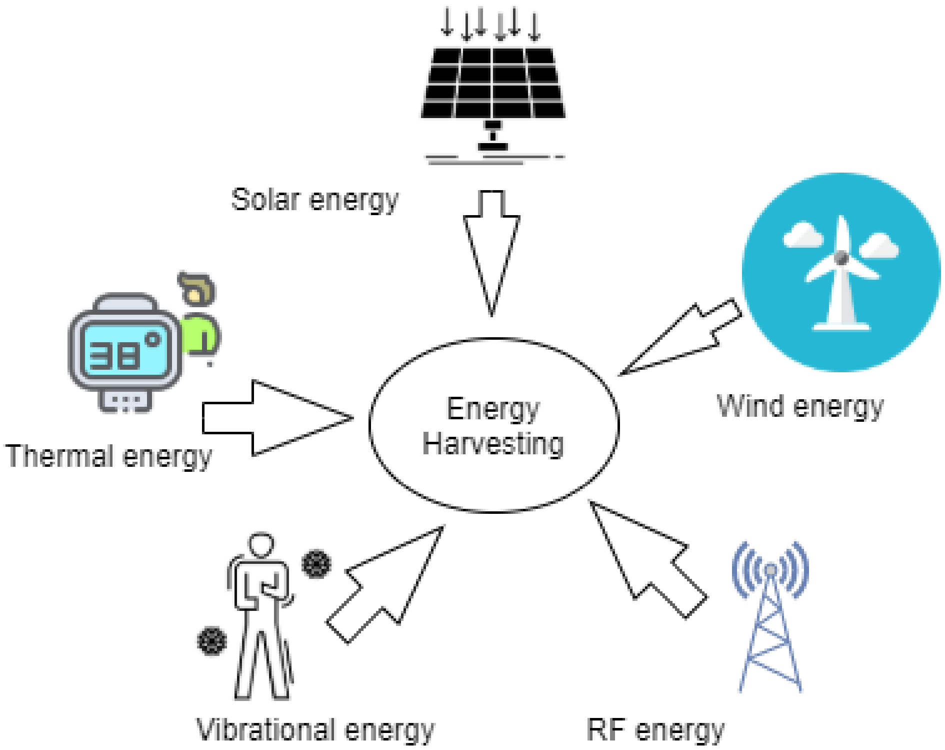

Figure 1.2: Commonly used sources for energy Harvesting.

Table 1.1: Characteristics of typical ambient energy sources.[1]

Characteristics	**Solar Energy**	**Thermal Energy**	**Ambient RF Energy**	**Vibrational Energy**
Power Density	100 mW/cm2	60 $\hat{A}\mu W/cm2$	0.0002 1 $\hat{A}\mu W/cm2$	200 $\hat{A}\mu W/cm3$
Available Time	Day Time (4 6 Hrs)	Continuous	Continuous	Activity Dependent
Pros	Large Amount of energy.	Always Available	Always Available	Light Weight
Cons	Non-continuous	Need large area, low power	Distance and Available power dependent	Variable power and Low conversion efficiency

With dedicated energy sources such as dedicated RF energy transmitter, the availability and amount of energy at a particular location is predictable. However, the amount of harvested energy is usually too small to power WSN components to meet these on-demand needs. Consequently, additional design considerations are needed to maximize the utility of systems using RF energy harvesters. In this thesis, we propose a mechanism that uses omnidirectional RF energy transmitter to power sensor nodes to transmit low-frequency updates, and a dedicated smart directional RF energy transmitter to a specific subset of nodes from which higher amounts of information is needed.

1.1 Motivation

R-EH involves collecting radio-waves through an antenna and converting it to electrical energy. The electrical energy is either used to recharge batteries or stored in super-capacitors and used by low power devices such as wireless sensors. Figure 1.3 illustrates typical RF energy harvesting setup in wireless sensor networks. Generally, it consists of a large number of wireless sensor nodes with energy harvesting capability, RF energy transmitters to energize them and a base station to receive the information transmitted by the sensor nodes.

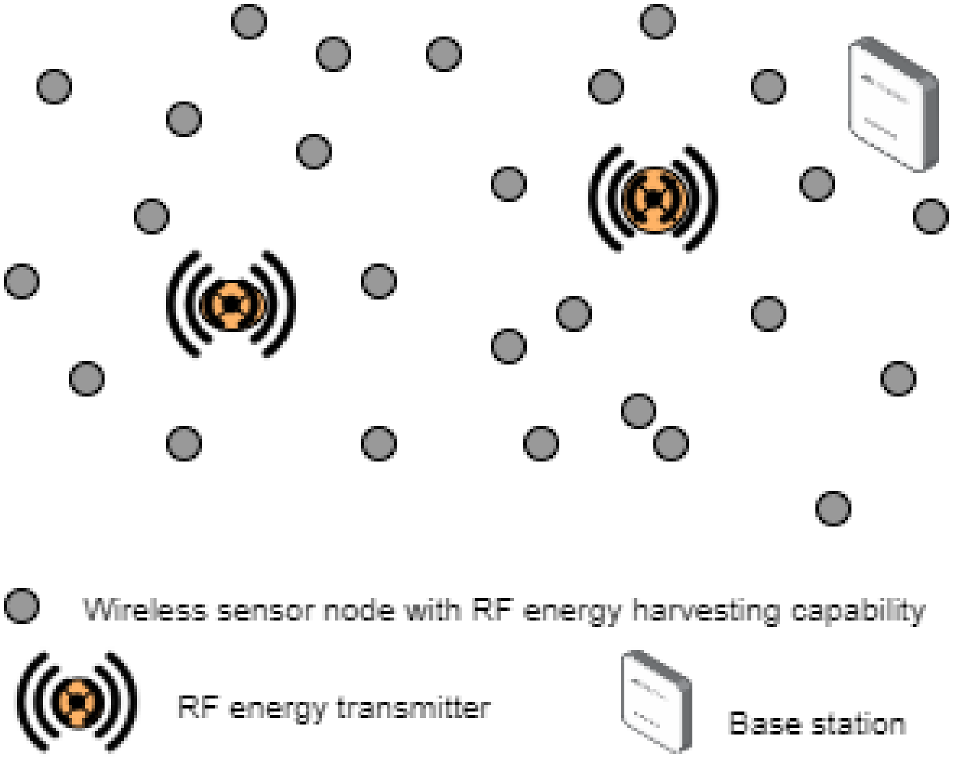

Figure 1.3: Typical RF energy harvesting in WSN.

RF energy transmitters could be omnidirectional or directional; however, they both have some limitations. Omnidirectional energy transmitters provide energy to a 360-degree area but sensor nodes need to be placed very near to energy transmitters to harvest energy. Directional energy transmitters can offer a longer range for harvesting energy but they cover a limited area. To a sensor node which is at the same distance from energy transmitters, the directional transmitter provides higher RF energy compared to the omnidirectional transmitter. We utilize this fact to deploy both the transmitters in combination in such a way that information from the network is maximized. The omnidirectional energy transmitter is used to energize the sensor nodes in the 360-degree area and they transmit information at some interval depending upon their distance from the transmitter, while directional energy transmitter is rotated to provide energy to a particular area where sensor nodes have significant information (such as an alarm indicating an occurrence of an abnormal event) to transmit at intervals shorter than that in omnidirectional transmitter case. Thus, the sensor nodes with an alarm condition get a chance to transmit at a faster rate such that the overall information from the network is maximized.

1.2 Contribution

In this work, an information-based smart RF energy harvesting scheme for wireless sensors networks is proposed, which uses a combination of an omnidirectional and a directional RF energy transmitter to cover a 360-degree (6 sectors of 60-degree) area by physically directing the antenna to serve the sensors that have the highest information content (alarms indicating an occurrence of abnormal events).

- Three different schemes are studied that differ on the energy transmitter combination (omnidirectional or both omnidirectional and directional) being used and corresponding rotation mechanism (sequential or maximum alarm based). Scheme-1 is the default scheme using omnidirectional antennas. Scheme-2 uses an omnidirectional and a directional antenna that rotated sequentially to cover 360 degree area. Finally, we propose a maximum alarm based directional transmitter rotation scheme to maximize the information from the network, scheme-3.

- The basic transmitter rotation scheme is implemented using Powercast corporation's wireless sensor development kit, and a servo motor based energy transmitter rotation mechanism. Due to hardware constraints, we used two sensor nodes with RF energy harvesting capability (a combination of energy harvester board and wireless sensor board), and a single directional energy transmitter to energize them. The servo motor based rotation mechanism points toward the sensor node which has generated the alarm.

- Additionally, the performance of the scheme with multiple sensor nodes and two energy transmitters (one omnidirectional and one directional RF energy transmitter) for different network scenarios are evaluated through extensive MATLAB simulations.

- A Markov's chain based information model is presented where events are modeled as a two-state Markov chain, the two states being normal and abnormal state. The probabilities of the occurrence of an abnormal event are varied to create different network scenarios and the probability of staying in the abnormal state is varied to create different cases in that network scenario.

- The simulation results analysis is presented based on total abnormal event captured by different schemes and average alarms generated per event as the probability of abnormal event occurrence and duration of the abnormal event is varied.

1.3 Thesis Outline

This section presents an outline of the thesis. In Chapter 2, the overview of RF energy harvesting techniques and related work in the area of RF energy harvesting is discussed. Chapter 3 presents the general overview of a dedicated RF energy harvesting system, hardware and software tools used for the implementation of schemes, preliminary results and observations for the Powercast wireless sensor development kit, and problem statement formulation based on the preliminary results. The proposed scheme setup, description of proposed schemes, and experimental setup to implement a basic transmitter rotation scheme are presented in Chapter 4. Chapter 5 presents the simulator setup, information model to model the abnormal events, and simulation parameters and assumptions. The simulation results and observations for different network scenarios and corresponding cases are presented in Chapter 6, followed by the conclusion and future scope of the work in Chapter 7.

CHAPTER 2: BACKGROUND AND RELATED WORK

2.1 Overview of RF Energy Harvesting

A radio frequency (RF) energy harvesting (R-EH) system consists of an RF energy source, an RF energy harvester, and a load used for the application. Radio frequency waves are an abundantly available source for energy harvesting, although it does require proximity to an RF transmitting antenna. Figure 2.1 illustrates the basic block diagram of a typical RF energy harvester.

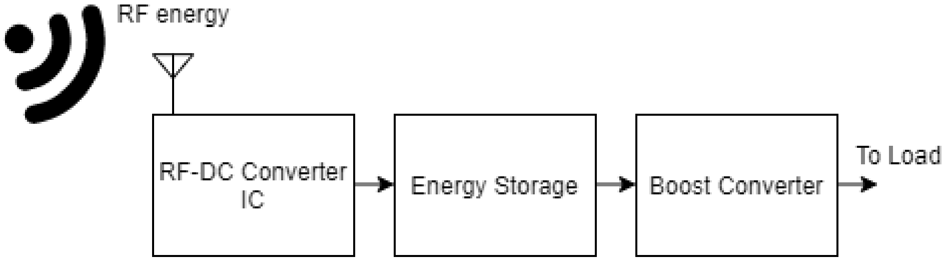

Figure 2.1: RF energy harvesting block diagram.

The RF energy can be generated from two origins: dedicated source and ambient source. RF energy is readily available from ambient sources such as cellular towers, WiFi, FM Radio, etc., but the availability of such sources and amount of energy available at a location are random. On the other hand, dedicated RF energy sources provide predictable and on-demand energy supply. The RF energy harvesting with dedicated sources is better suited for applications with quality of service constraints. Harvesting energy from RF is not a new concept and the process is quite simple. Radio waves reach an antenna that is tuned to that frequency and cause a changing potential difference across its length. The potential difference across the length of the antenna causes charge carriers to move along the length of the antenna in an attempt to equalize the field. The RF-to-DC conversion integrated circuit captures energy from the movement of those charge carriers and RF energy is converted to DC. The energy is then stored temporarily in a capacitor, when a charge threshold on the capacitor is achieved, the voltage is boosted to the set output level and supplied to the load as and when required. The RF-to-DC converter IC generally is a combination of an impedance matching circuit and a rectifier circuit. A boost converter is a DC-to-DC step up converter that provide a output voltage greater than source voltage.

The amount of energy harvested depends on the received RF energy which in turn depends on the transmitted RF energy from an RF source. Under idealized conditions, the relation between transmitter power and received power is given by Friis's free space equation 2.1

$$P_R = G_t G_r (v/4\pi d)^2 P_T \tag{2.1}$$

where $\mathrm{P_R}$ is the received RF power, d the distance between the receiver and the source power $\mathrm{P_T}$, $\mathrm{G_T}$ the source antenna gain, $\mathrm{G_R}$ the receive antenna gain, and v the wavelength of the carrier frequency.

However, the received electrical power depend on the RF-to-DC conversion efficiency of the RF-to-DC converter. The relation between the received RF power and the electrical power after conversion is given as:

$$P_R^{DC} = (\eta_{RF-DC}) P_R \tag{2.2}$$

where $\eta_{\mathrm{RF\text{-}DC}}$ is RF to DC conversion efficiency and $\mathrm{P_R}$ is received RF power, $\mathrm{P_R}^{\mathrm{DC}}$ is converted electrical power.

It is very easy to design a system capable of RF energy harvesting utilizing various combinations of power management ICs (PMICs), power receiver chips, Antennas, energy transmitters, etc. Powercast, E-peas, COTA, and WattUp currently provide commercial solutions and use specialized integrated circuits (ICs) designed specifically for high efficiency RF-to-DC conversion. A more detailed RF energy harvesting process and hardware description of Powercast RF energy harvesting for wireless sensor network kit is presented in next chapter.

2.2 Related Work

RF energy harvesting has attracted a lot of attention from researchers working in the area of low power devices. R-EH not only provide battery-free operation of low power devices, but it could also be used to charge batteries for uninterrupted and prolonged operation. Several studies reported the utilization of ambient RF energy to harvest energy. [2], [6], [8] present the survey of various energy harvesting techniques and provide details of the RF energy harvesting technique. The authors of [9] present a study on the feasibility of ambient RF energy harvesting for low power device operation. On the same lines, a lot of work has been done towards prototype implementation of ambient RF energy harvesting. A survey on hardware design issues in RF energy harvesting is presented in [10]. In [11], the authors have developed a prototype to harvest energy from TV broadcast airwaves.

The amount of energy harvested from radio waves depends on the conversion efficiency of RF-to-DC converter circuit which is called rectenna (rectifying antenna), a diode based circuit that converts RF to DC. Several rectenna designs and architectures that maximize the conversion efficiency in different frequency bands have been proposed in [12],[13]. In [14], the authors propose a rectenna array to further boost the RF-to-DC conversion efficiency. The conversion efficiency reduces sharply at low input RF power due to nonlinearity in the diode characteristics. For low RF input, diodes with low turn-on voltage are used in voltage multiplier circuit. A two-state design was presented in [15], that works well with both low input RF power and higher input RF power. For low input RF power, a seven stage voltage multiplier design and a ten stage multiplier circuit for higher input RF power was proposed. Inserting a transitional DC-to-DC converter with peak power tracking that can reconfigure the DC load of rectenna array with varying input RF power, to maximize the DC power generation was proposed in [16].

Simultaneous transfer of information and energy is another research area in RF energy harvesting. In [17], authors have presented two practical approaches for simultaneous energy and information transfer. One is time switching where dedicated time slots are allocated for energy and information transfer. The other is power splitting where one part of received signal is used for RF energy harvesting and the other part is used to decode the information. The authors in [18], have investigated the outage probability performance and the average harvested energy when power splitting is used for simultaneous energy and information transfer for a large scale network. In [19], the authors presented different antenna array configuration for simultaneous energy and information transfer. They used two antennas for energy reception and one antenna for information exchange, to minimize the interference between energy and information transfer and provide some beam-forming.

The energy transfer with a antenna with omnidirectional radiation pattern undergo serve path loss as the transmission distance increases because of beam spreading. The method in RF energy harvesting where the RF waves are concentrated, via multiple antennas, in a direction is called energy beam-forming which was first used in [17] for simultaneous energy and information transfer in multiuser downlink. In [20], the authors have investigated the joint optimization of transmit power control, information and power transmission scheduling assuming perfect channel state information at the transmitter. A directional RF energy transmission scheme is proposed in [21] to overcome the path loss and increase the reception distance. The authors in [22], demonstrated that a higher energy transfer efficiency can be achieved through energy beam-forming based on accurate channel state information. But the longer time required to extract accurate channel state information shortens the energy transfer duration, resulting in less harvested energy. In [23], the authors have presented a detailed study on research in beam-forming and, simultaneous energy and information transfer. They present the challenges in feasibility of RF energy harvesting, new research directions, and obstacles to their practical implementation.

Researchers have used commercially available Powercast Corporation's energy transmitters and development kits for experimental studies, feasibility tests of ambient sources, hardware design, and designing applications. In [24], an experimental approach is presented for RF energy harvesting in wireless sensor networks for critical aircraft monitoring systems. In our earlier work [25], we proposed a directional transmitter rotation scheme for information maximization. In [26], authors investigate the impact of the usage of different waveforms on the efficiency of wireless power transfer (WPT) to the Powercast device. The investigation was done at sub-GHz frequencies and conversion of the average transmitted and received power at the output of harvesting device into DC power was analyzed. An experimental approach to reduce power consumption at the energy transmitter side was presented in [27] by turning off and on the energy transmitters. [28] presents an outdoor dust monitoring application using the Powercast energy transmitter. A similar approach was used to develop an RF energy harvesting system for Li-Fi application in [29]. The authors in [30] have presented an empirical model based on an experimental setup for a mobile charging scheme using a Powercast kit. They use a mobile charging station that can travel through a preplanned path to charge the sensor nodes in that area. Also, they proposed an optimal policy for the RF energy transmitter to select a path to schedule the charging for all the sensor nodes.

CHAPTER 3: SYSTEM DESCRIPTION

We use a commercially available R-EH development kit manufactured by Powercast [31], which consists of one RF transmitter (TX-91501-3W), two harvesting boards (P2110), two wireless sensor boards that can be attached on top of harvesting board, two 6 dBi antennas, and an access point. Figure 3.1 shows the components of the Powercast development kit.

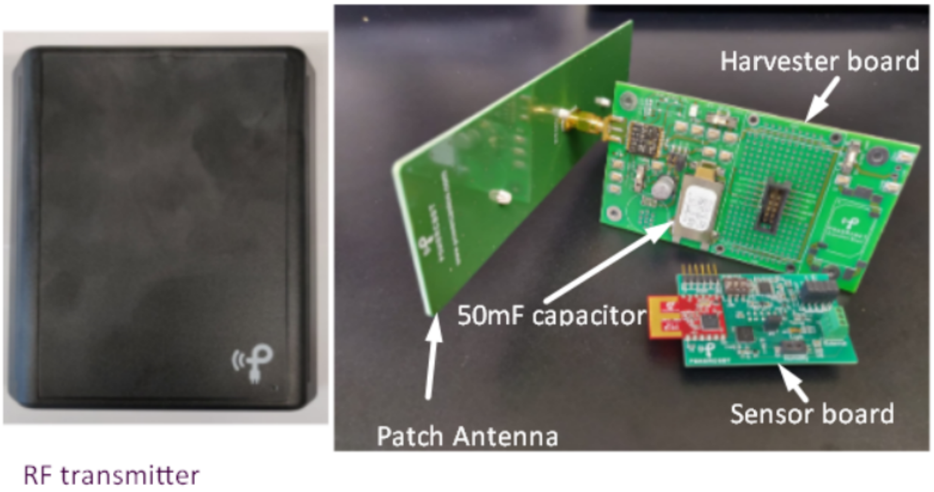

Figure 3.1: Powercast WSN development kit.

The transmitter (TX91501B) radiates RF energy at 915 MHz with an integrated 8 dBi antenna and is capable of simultaneous wireless power and information transfer[31]. The power is transmitted using direct sequence spread spectrum (DSSS) and data is transmitted with amplitude shift keying (ASK) modulation. Currently, it transmits only preprogammed transmitter ID along with RF energy. The output power of the energy transmitter is 3 Watt (EIRP). The RF energy beam pattern has width with 60 degree and height of 60 degree, and has vertical polarization.

The Powerharvester receiver (P2110) receives RF energy through a patch antenna connected via an SMA connector. The patch antenna is 915 MHz directional antenna with 120-degree reception pattern. The powerharvester converts RF energy to a DC voltage and stores it in a capacitor. It contains a 1 mF (C3) and a 50 mF (C5) capacitor on board as well additional capacitors can be added for testing. When a threshold voltage of 1.25 Volts, across the charge capacitor is reached, the P2110 boosts the voltage to 3.3 Volts and enables the power supply out. The Vout voltage remains steady at 3.3V as long as the voltage across the capacitor Vcap remains above 1.05 Volts. Figure 3.2 displays timing diagram of the P2110.

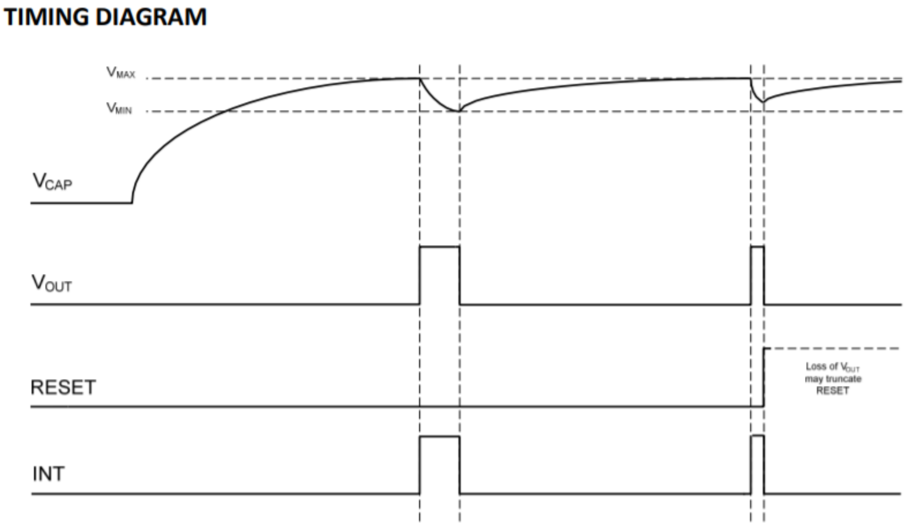

Figure 3.2: Timing diagram for P2110 [31] .

The wireless sensor board has humidity, temperature, and light sensors and an additional sensor can be attached through a terminal block near the edge of the board. A Microchip PIC24F16KA102 microcontroller is used to enable sensors to read and process sensed data, and send it to the transmitter. When voltage Vout is above a certain value i.e 3.3 Volts, the sensor board turns on, the sensors read data and process it, and transmit it via an MRF24J40MA RF Transceiver Module to the access point. The sensor board of the P2110-EVAL-1 kit comes with a preloaded firmware in C language and requires Microchipâs MPLAB IDE and C30 Compiler. The default firmware settings include a reset signal that turns off Vout after the packet data are transmitted.

The Microchip XLP 16-bit development board with a Microchip MRF24J40 PICtail attached is used as the access point of the system. The sensor board communicates with the access point at a frequency of 2.4 GHz using a protocol that is implementing the IEEE 802.15.4 standard [31]. The preloaded firmware can be modified and, sensor board and access point are reprogrammed using PICtail programmer.

In addition to the Powercast WSN development kit, Texas Instrument's TIVA C series board and Hitec HS-422 servo motor are used for implementing rotation mechanism. More details of rotating mechanism implementation are provided in the experimental setup section in Chapter 4.

3.1 Hardware Setup and Customization for Powercast Kit.

To understand the working, energy usage, and energy harvested at different distances, out of box experiments were conducted on Powercast kit. Figure 3.3 demonstrates the basic setup for out of box evaluation.

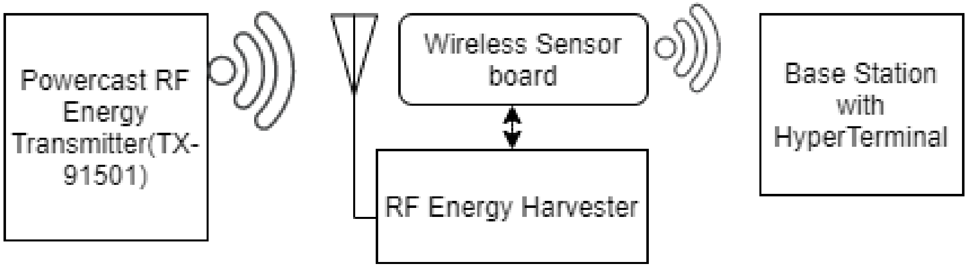
Powercast RF Energy Transmitter(TX-91501)
Wireless Sensor board
RF Energy Harvester
Base Station with HyperTerminal

Figure 3.3: Basic setup for out of box experiments.

In default mode, when power is available to the sensor node, it performs sensing and transmits the data to the access point. At the end of the transmission, the sensor board resets the harvester. After a delay of 10 seconds, the process is repeated, provided the voltage of 3.3 volts is available continuously to the sensor node [31]. In practice, leakages in the harvester board cause the voltage across capacitors to drop below a threshold of 1.02 volts before completion of the 10 seconds delay, which shuts down the boost converter and the supply to the sensor node is cut off. Hence, it starts new sensing and transmission at intervals longer than 10 seconds. The mode of operation was modified to analyze the energy usage in other modes such as single sensor operation, no reset operation, no transmission operation, etc. The results of their experiments are presented in the preliminary results section.

3.2 Preliminary Results and Observations

We present preliminary results of energy available from the RF energy harvester and energy usage at the sensor nodes under different conditions. Figure 3.4 shows the received signal strength indicator (RSSI) at various distances from the transmitter in default mode. The corresponding intervals between successive transmissions from the harvested energy in default mode are shown in Figure 3.5.

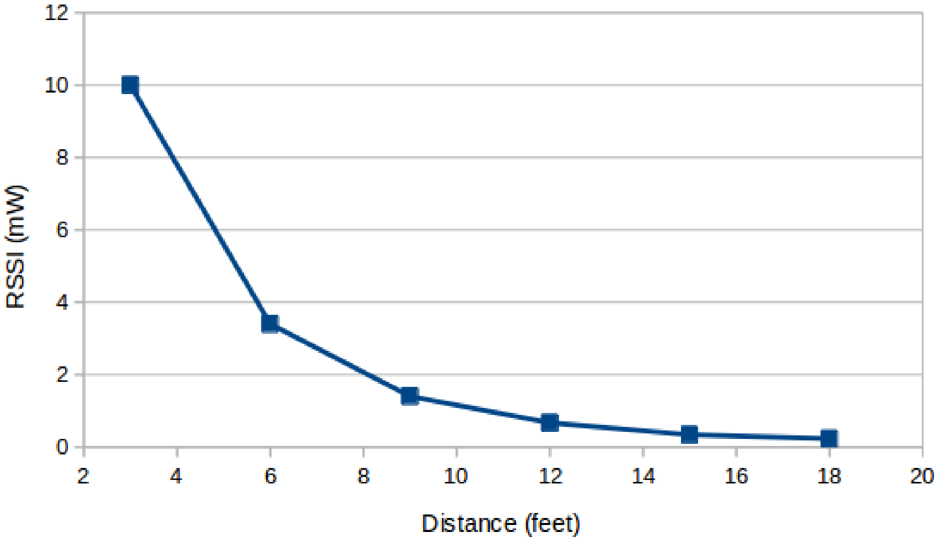

Figure 3.4: RSSI variation with distance for default mode.

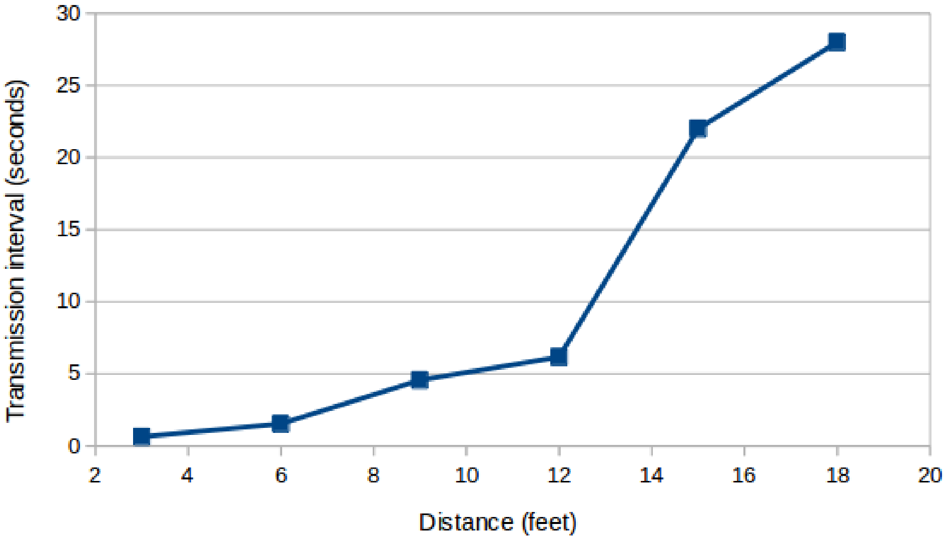

Figure 3.5: Transmission interval variation with distance.

The energy used in the sensor board depends on its mode of operation. In the default mode of operation, all the sensors in the board are activated and the harvester board is reset after every packet transmission and reinitialized. We programmed the sensor for operating under different numbers of active sensors with the LED turned ON and OFF without resetting the harvester, each of which draws a different amount of current. As the capacitor in the harvester is discharged, the voltage across it V cap drops, and eventually the output voltage Vout of the harvester is cut off. Figure 3.6 and Figure 3.7 depict the variations of Vout and Vcap for two specific cases with the LED OFF. Table 3.1 provides the observed duration of Vout for different cases.

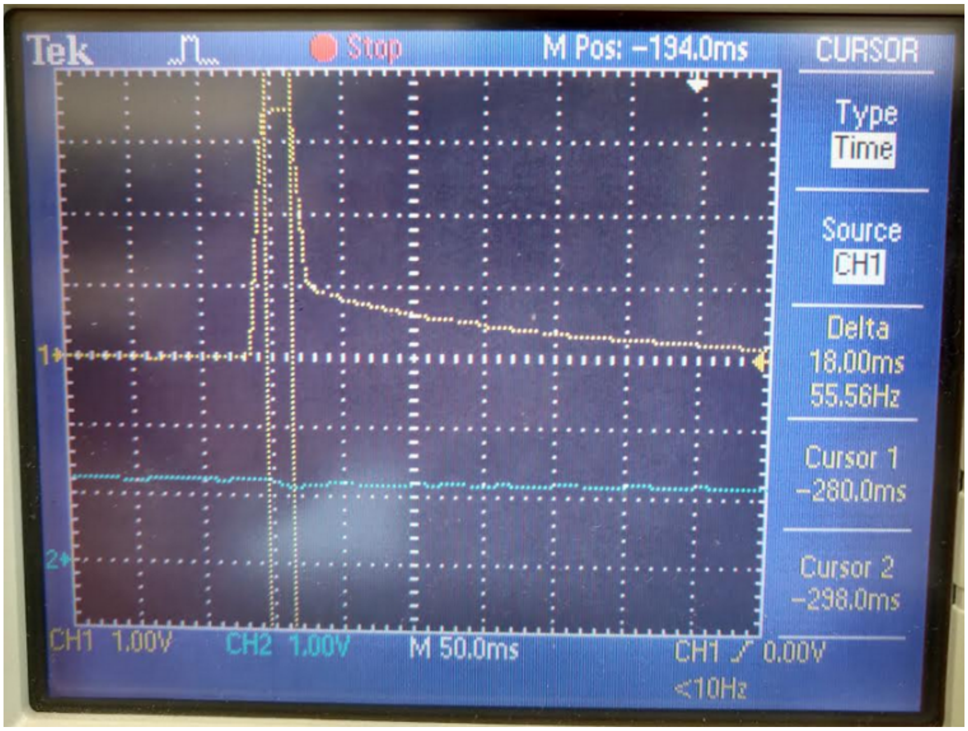

Figure 3.6: Vout and Vcap with all sensors activated with reset.

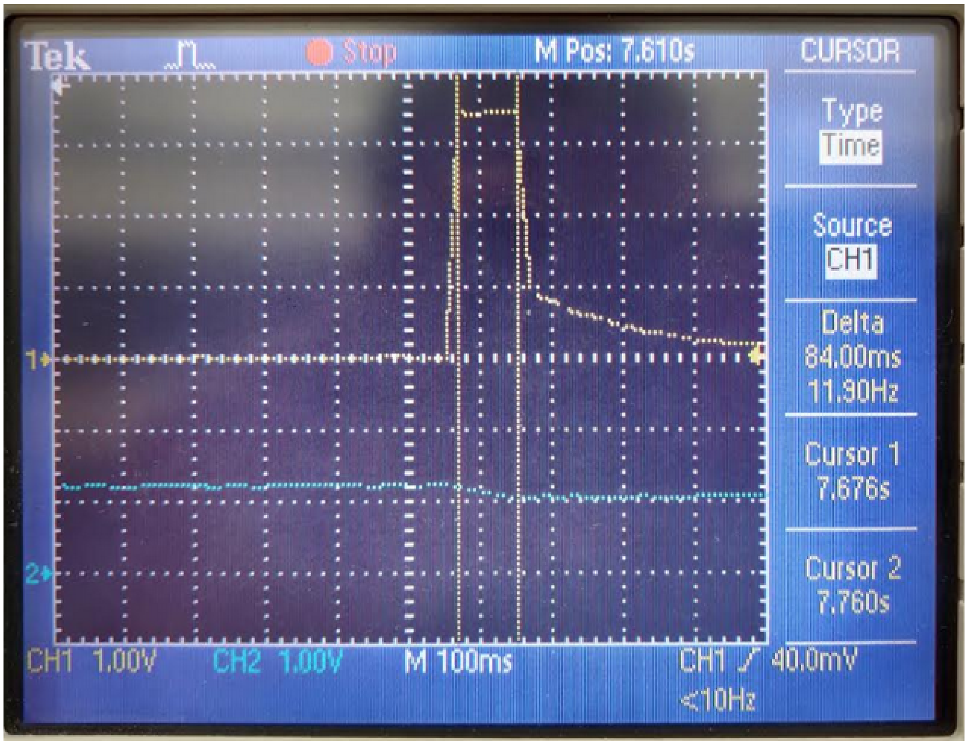

Figure 3.7: Vout and Vcap with all sensors activated with no reset.

Table 3.1: Duration of V out for different use cases.

Use cases	With LED	Without LED
Without sensor board	180 ms	9.2 seconds
Default operation	18 ms	20 ms
1 sensor + transmission	92 ms	200 ms
All sensors + transmission	52 ms	84
All sensors + no transmission	88 ms	190 ms

The Vout interval changes as we change the distance of harvester from the energy transmitter. Table 3.2 presents Vout interval and Vout duration for no-load condition. The observations in different modes of operation help us to design a harvesting system to effectively utilize the harvested energy. Table 3.3 presents the interval and duration of Vout when only the light sensor is on, all other sensors, RSSI calculation, voltage measurement, TX ID circuit is off and no reset after transmission. Table 3.4 presents the interval and duration of Vout when only the light sensor is on, all other sensors, RSSI calculation, voltage measurement, TX ID circuit is off and reset after transmission. Table 3.5 presents the interval and duration of Vout when all sensors are on, and no reset after transmission.

Table 3.2: Interval and duration of Vout for no load condition.

Distance(feet)	Interval of Vout	Duration of Vout
3	11.6 seconds	9.2 seconds
6	13.6 seconds	9.2 seconds
9	26.2 seconds	9.2 seconds

Table 3.3: Interval and duration of Vout for only light sensor on and no reset.

Distance(feet)	Interval of Vout	Duration of Vout
3	2.8 seconds	240 ms
6	3.2 seconds	240 ms
9	12 seconds	240 ms

Table 3.4: Interval and duration of Vout for only light sensor on and reset.

Distance(feet)	Interval of Vout	Duration of Vout
3	240 ms	12 ms
6	380 ms	12 ms
9	2.4 seconds	12 ms

Table 3.5: Interval and duration of Vout for all sensors on and no reset.

Distance(feet)	Interval of Vout	Duration of Vout
3	2.2 seconds	180 ms
6	3.6 seconds	180 ms
9	22 seconds	180 ms

3.3 Problem Statement Formulation

In this section, we analyze the preliminary results is presented and present a problem statement based on the analysis. In the preliminary result section, variations of RSSI and transmission interval with distance for the default mode is presented. Also, the sensor nodes are programmed to operate in modes other than default mode to study energy usage and the corresponding transmission intervals in those modes. In default mode, the sensor nodes send a reset signal to the harvester board which in turn stops 3.3 Volts supply to the sensor node. This helps the harvester board to save stored energy and charge faster as the charging time depends on the residual charge in the supercapacitor. In other modes the sensor node's current consumption depends on the number of sensors enabled and functions performed. If we mask the reset option, the Vout duration increases enabling sensors to perform more tasks. In single sensor operation (light sensor), sensor board transmitted twice in a single harvesting cycle with a delay of 10 ms between to successive transmissions. As the duration of the Vout increase without the reset option, the successive transmission interval also increases because the residual charge becomes zero and harvester takes more time to charge the supercapacitor again. This difference in the successive transmission interval becomes significantly larger as the distance between the energy transmitter and harvester board increases.

In light of the above analysis, it can be concluded that in terms of successive transmission interval, the default mode operation is better as compared to other modes provided a continuous RF energy is available to the harvester board. As we use an on-board 50 mF capacitor to store charge, this charge is not enough for prolonged operation even in the least power consuming operation mode. In order to prolong the sensor operation duration, a higher value capacitor needs to be used. But, this will take more time to charge.

To provide a solution to the above problems, the use of two energy transmitters (one omnidirectional and one directional) and operating sensor node in default mode is proposed. This enables the harvester board to charge the supercapacitors continuously and default mode operation enables sensor nodes to transmit frequently. Although omnidirectional transmitters can provide energy to a smaller area compared to directional energy transmitter, they both can be deployed together to provide periodic updates from sensors in all the direction and multiple intermediate updates from the direction to which directional transmitter is facing. The schemes description and experimental setup to demonstrate the proposed scheme are provided in the next chapters.

CHAPTER 4: PROPOSED SCHEME AND EXPERIMENTAL SETUP

4.1 Proposed Scheme for Transmitter Rotation

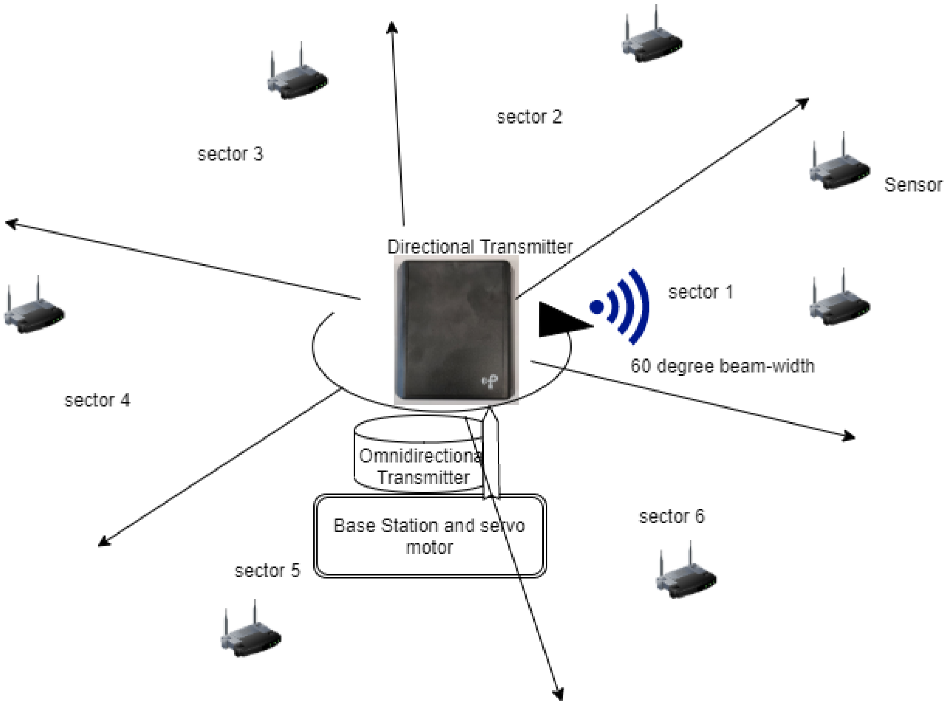

Figure 4.1: Scheme setup.

Figure 4.1 illustrates the system setup for transmitter rotation. This setup consists of an omnidirectional and a directional RF energy transmitter to cover a 360-degree (6 sectors of 60-degree) area. The setup considers an alarm monitoring application where the sensor nodes harvest RF energy from the omnidirectional energy transmitter and transmit sensed information periodically. If the sensed value crosses a certain threshold, the access point(base station) generates a flag of value 1 for that node. The flags with value 1 are considered as alarms. When the most distant node provides a periodic update, alarms from all the sectors are counted and the directional energy transmitter is directed to a sector that has maximum alarms.

We define three schemes based on the assumed energy transmitters used (i.e. omnidirectional only or both omnidirectional transmitter) and the rotation mechanism of the directional transmitter i.e. (sequential or maximum alarm based). The details and flow diagrams of the three schemes are described below.

Scheme 1: Single omnidirectional energy transmitter deployed to energize all sectors in order to provide periodic updates from all sensor nodes. The sensors in each sector will take time to harvest enough energy depending on their distance from the RF energy transmitter and the radiated energy from the transmitter. With a single omnidirectional transmitter, the sensor nodes will provide periodic updates only. Figure 4.2 demonstrate scheme 1 flow diagram.

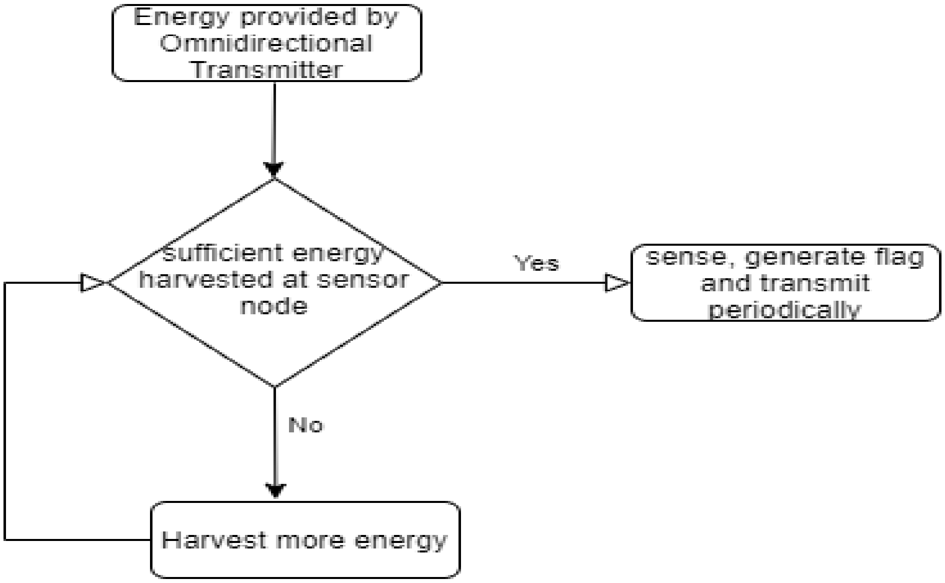
Energy provided by Omnidirectional Transmitter
sufficient energy harvested at sensor node
Yes
sense, generate flag and transmit periodically
No
Harvest more energy

Figure 4.2: Scheme 1 flow diagram.

Scheme 2: One omnidirectional and one directional energy transmitter are deployed to provide periodic updates from all sectors and intermediate updates from a single sector which is energized by the directional transmitter. After periodic updates from most distant nodes, the directional transmitter moves sequentially from sector 1 to sector 6 and then comes back to sector 1 to start again. Figure 4.3 demonstrate scheme 2 flow diagram.

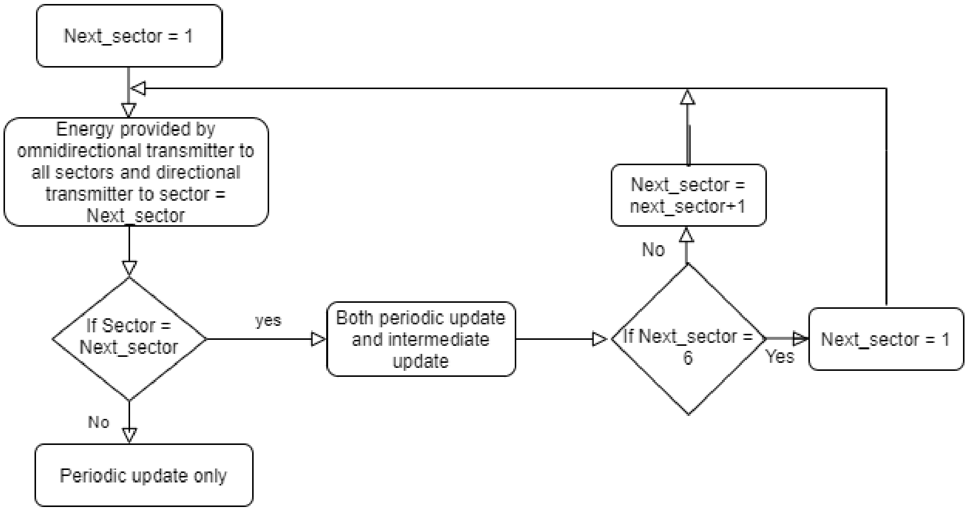
Next_sector = 1
Energy provided by omnidirectional transmitter to all sectors and directional transmitter to sector = Next_sector
If Sector = Next_sector
yes
Both periodic update and intermediate update
If Next_sector = 6
Yes
Next_sector = 1
No
Next_sector = next_sector+1
No
Periodic update only

Figure 4.3: Scheme 2 flow diagram.

Scheme 3 (Proposed Scheme): After a periodic update from the most distant node, the total alarms (flag value 1) from all sectors are counted and the directional transmitter is moved to the sector with the maximum number alarms. Figure 4.4 demonstrate scheme 3 flow diagram.

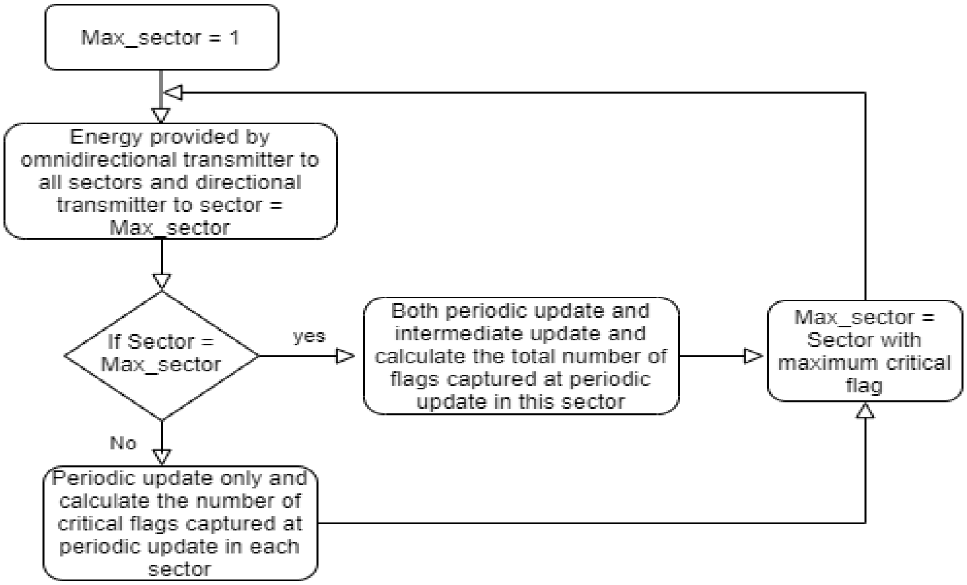
Max_sector = 1
Energy provided by omnidirectional transmitter to all sectors and directional transmitter to sector = Max_sector
If Sector = Max_sector
yes
Both periodic update and intermediate update and calculate the total number of flags captured at periodic update in this sector
Max_sector = Sector with maximum critical flag
No
Periodic update only and calculate the number of critical flags captured at periodic update in each sector

Figure 4.4: Scheme 3 flow diagram.

4.2 Experimental Demonstration

Due to hardware constraints, the above proposed scheme's demonstration was done using two sensor nodes (representing two sectors), one directional (representing omnidirectional transmitter) and a servo motor based rotation mechanism to point towards the the direction of the sensor node that that generated the alarm (representing directional transmitter rotation to the sensor that generated alarm). The reduced set up of figure 4.1 for experimental purpose is illustrated in figure 4.5.

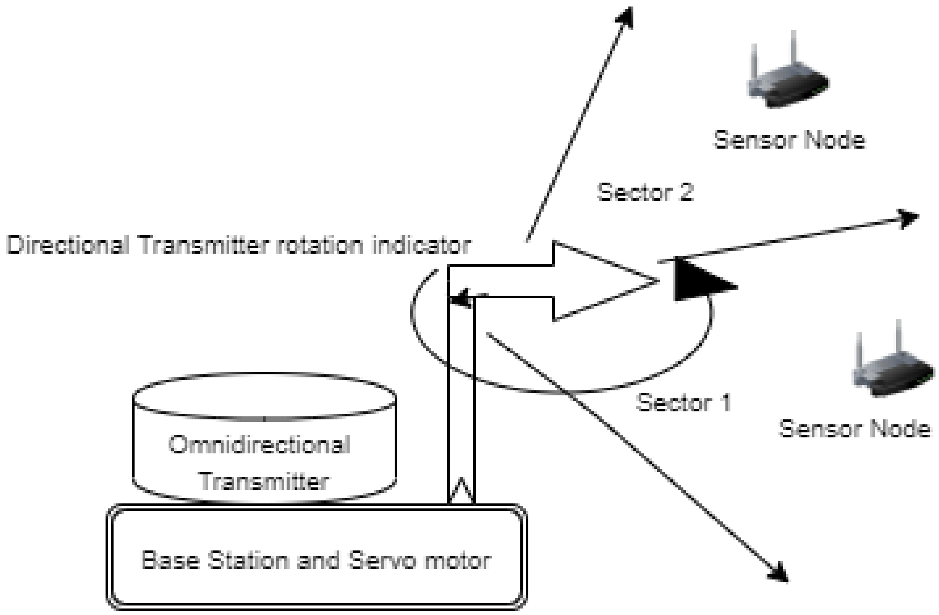
Sensor Node
Sector 2
Directional Transmitter rotation indicator
Sector 1
Sensor Node
Omnidirectional Transmitter
Base Station and Servo motor

Figure 4.5: Reduced scheme setup.

Figure 4.6 illustrates the experimental setup for implementation. Powercast corporations WSN development kit for RF energy harvesting, TIVA C series microcontroller, and servo motor is used for the implementation. A 3 Watt Powercast transmitter provides RF energy to the harvester board which harvests energy and supplies it to sensor nodes. Light sensors are used to create an abnormal event occurrence by placing hand over it. The sensor boards operate in default mode i.e. they reset the power supply to enable harvester board to charge faster. Once the voltage across the capacitor crosses the value of 1.25 Volts, the boost converter provides 3.3 Volts to sensor boards. The sensor board, on receiving 3.3 Volt supply, enables light sensors to sense the intensity of the light and transmit the information to the access point which serves as a base station. if the sensed value lies outside a predefined threshold, the access point generates a flag with value 1 for corresponding sensor node.

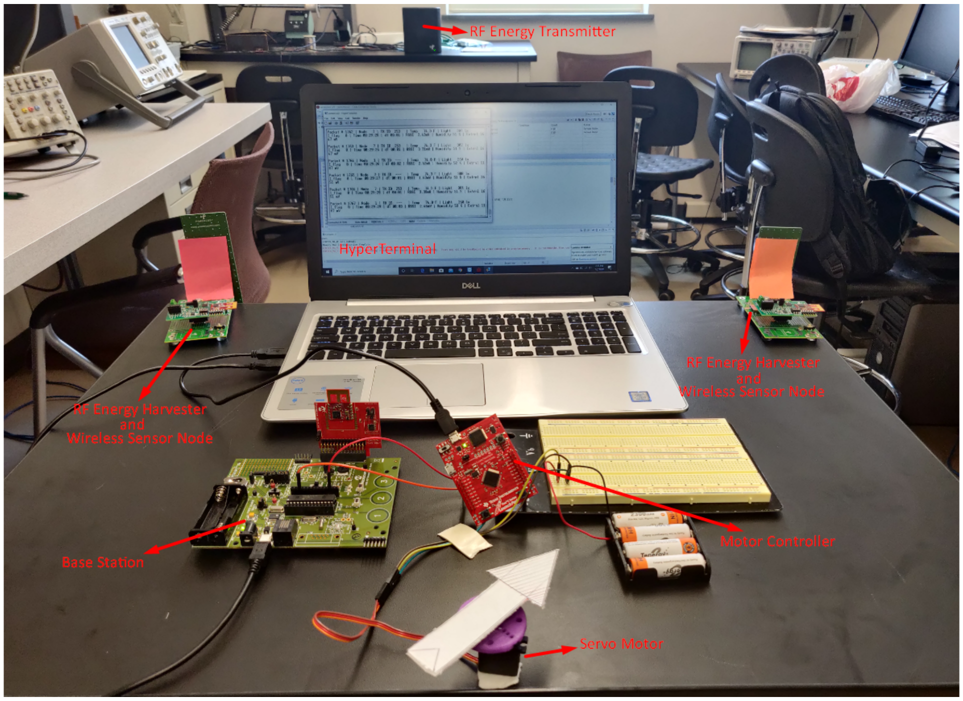
RF Energy Transmitter
HyperTerminal
RF Energy Harvester and Wireless Sensor Node
RF Energy Harvester and Wireless Sensor Node
Base Station
Motor Controller
Servo Motor

Figure 4.6: Experimental Setup for scheme implementation.

The flags with value 1 are considered as alarms indicating the occurrence of an abnormal event. The abnormal events are crated by placing hand over the light sensor to change the light intensity. When the base station generate an alarm for a sensor node, it glows a LED corresponding to that sensor node to show the occurrence of an abnormal event at that sensor node location. As discussed earlier, due to hardware constraints, Only a directional energy transmitter and two sensor boards are used for the experiment. We denote one sensor node as Node-red and other as Node-orange. When an alarm is generated for Node-red at the base station, the red LED on the base station glows. Similarly, when an alarm is generated for Node-orange, the orange LED on the base station glows. The actual sensed value, node ID, Transmitter ID, and flag values are displayed in the HyperTerminal connected to the base station.

The base station sends alarm information to a motor driver. In this setup, we have used the TIVA C series microcontroller to drive the servo motor. The motor driver is programmed to provide PWM pulses to the servo motor to rotate to the direction of the sensor node that generated the alarm. The light intensity value is changed by placing hand above the light sensor and alarms are generated. The LED corresponding to the sensor node generating alarm glows and the servo motor rotates to the direction of that sensor node.

CHAPTER 5: PERFORMANCE EVALUATION USING SIMULATION

5.1 Simulation Setup

To evaluate the performance of the information based rotation scheme of the directional transmitter with multiple sensors MATLAB simulations were used with certain assumptions. Simulation considers a combination of one omnidirectional RF energy transmitter and one directional RF energy transmitter with a 60-degree beamwidth. Omnidirectional RF energy transmitter provides energy to all the sectors equally covering 360-degree area and directional RF energy transmitter provides the energy to a sector covering 60-degree area.

It considers a network with 6 sectors and 9 sensors in each sector. In a sector, three sensor nodes placed at the circumference of each concentric circles namely Z1, Z2, and Z3. Figure 5.1 demonstrate the system setup for simulation. The relative harvesting times with omnidirectional and directional energy transmitters as depicted in figure 5.2 are chosen arbitrarily assuming that the total radiated RF power is same in both cases and the beamwidth of the directional antenna provides 2.4 times more RF power (considering equal distribution of RF radiated power in both the antennas) such that the corresponding harvesting time with combination of both the transmitters is three times less as compared to with only omnidirectional antenna and with same total radiated RF power.

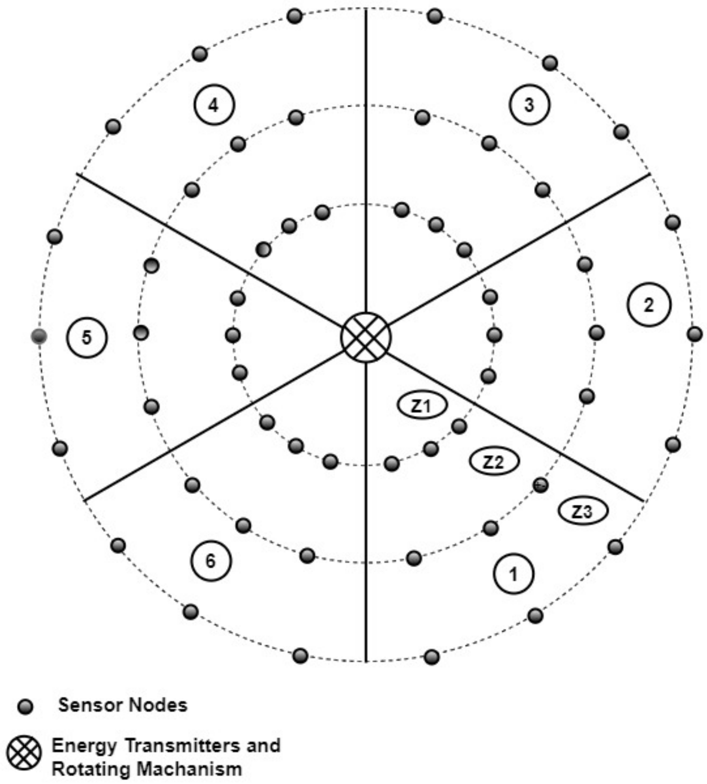

Figure 5.1: Simulation setup.

The omnidirectional transmitter will energize the sensors to provide periodic updates from all sectors and the directional transmitter will provide the energy for intermediate updates in addition to periodic updates from a single sector. When deployed together, they will provide periodic updates from all sectors and intermediate updates from a single sector. The effective isotropic radiated power (EIRP) of the omnidirectional antenna is assumed such that the sensor nodes at different distances take a certain time to harvest energy and transmit the information. It is assumed that the node which are equidistant from energy transmitter take same time to harvest energy. With a combination of omnidirectional and directional energy transmitter, the sensor nodes take less time to harvest energy. For the simulation, this time is assumed to be three times less as compared to that take with only omnidirectional energy transmitter.

Figure 5.2 illustrates the alarm generation by the sensor nodes located in different zones, when only omnidirectional energy transmitter is used and when both omnidirectional and directional energy transmitters are used. Whenever the physical entity is in the abnormal state the sensor nodes generate an alarm at time instances depending on their distance from energy transmitters, and the energy transmitter combination being used to energize them. We consider discrete time slots of duration 't' to represent the energy harvesting time and, processing and transmission time required by sensor nodes. Specifically, with single omnidirectional transmitter deployment, we assume that the sensor nodes on circle Z1 take six time slots to harvest energy, process the information, and transmit with or without alarm depending on the state of physical entity. Similarly, the sensor nodes on circles Z2 and Z3 take twelve time slots and twenty four tome slots respectively for the same. The gray shaded rectangular box represents sensor node processing time after sufficient energy is harvested. The sensor node transmit the processed information and if there is an alarm condition, it is indicated by arrow sign over the rectangular box.

When omnidirectional and directional transmitters are used in combination, the sensor nodes on circle Z1, take two time slots to sense, process and transmit the information. In the same way, the sensor nodes on circles Z2 and Z3 take four and eight time slots respectively for the same. Also, it is assumed that the transmitted information is received by the base station instantly. The decision to move the directional energy transmitter is taken after each twenty four time slots which is the time required for nodes at Z3 (most distant nodes) to transmit information.

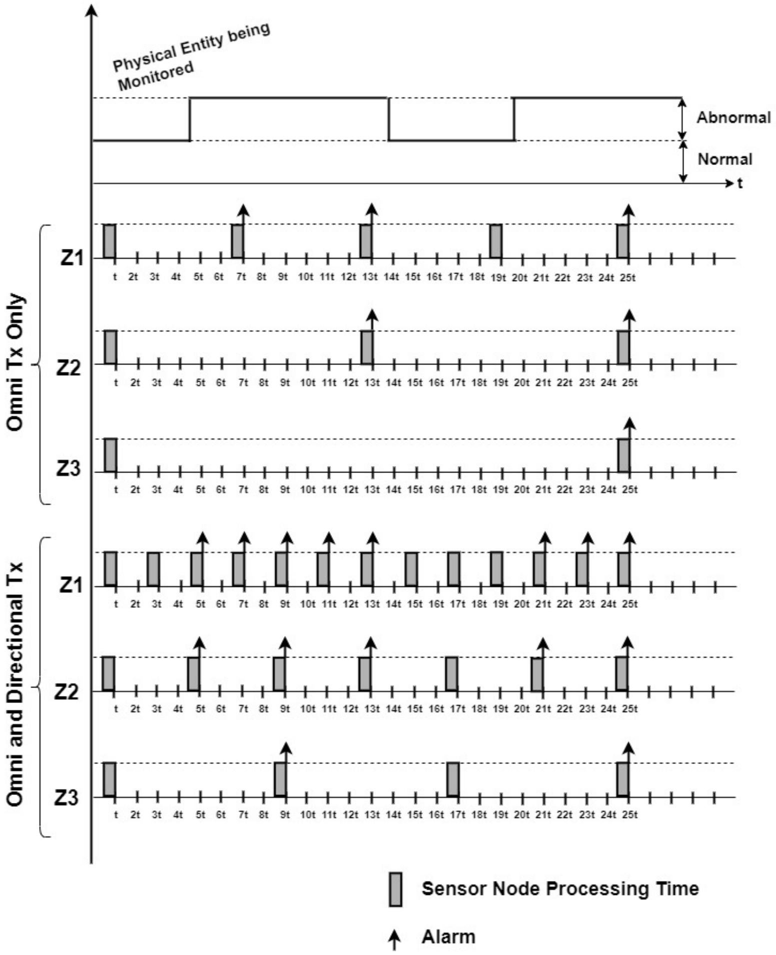

Figure 5.2: Energy harvesting time and alarm generation.

5.2 Information Model

An appropriate information model is developed to generate the sensing data i.e. physical entity being monitored by the sensor node and the flag generation scheme with following assumptions. The sensing data values are classified into two states. One is a normal state where data values are in an acceptable range and the other is an abnormal state where the data values are beyond the threshold value. The sensing data varies around a mean with a small fixed variance in the normal state of operation. In the abnormal state of operation, the sensing data varies around a different mean which is higher than that of the normal state but with the same variance. In general, the system is mostly in the normal state, but if some event occurs then the system moves to the abnormal state and stays there for some time. However, the duration for which it stays there varies differently for different events. There may be a few sudden state changes and the future states depend only on the current state and not on the events that occurred before it.

5.2.1 Markov chain-based state transition model

A Markov's chain is a stochastic model that describes a sequence of possible events according to certain probabilistic rules. In continuous-time, it is known as Markov's process, named after the Russian mathematician Andrey Markov. This stochastic process satisfies Markov's property i.e. memorylessness. The future states or outcomes in a Markov's chain depends solely on the current state and is independent of the states that have occurred before it. Markov's chains find many applications in statistical modeling of real-world processes such as queue/lines of customers arriving at an airport, weather condition modeling, etc. We use a two-state discrete-time Markov's Chain to model a sequence of normal and abnormal events.

Figure 5.3 demonstrates a two-state Markov chain. The probabilities of state transitions depend on the present state. State 1 is a normal state and state 2 is an abnormal state. The flags are generated with value 0 when the current state is 1 and when it moves to state 2, the flags are generated with value 1. When a sensor node generates a flag with value 1, it is considered as an alarm indicating the occurrence of an abnormal event. The probability of state transition from the normal state to abnormal state is defined as alpha and the probability of state transition from abnormal state to the normal state is defined as a beta. The value of alpha decides the number of occurrences of abnormal events and the value of beta decides the duration of the abnormal event.

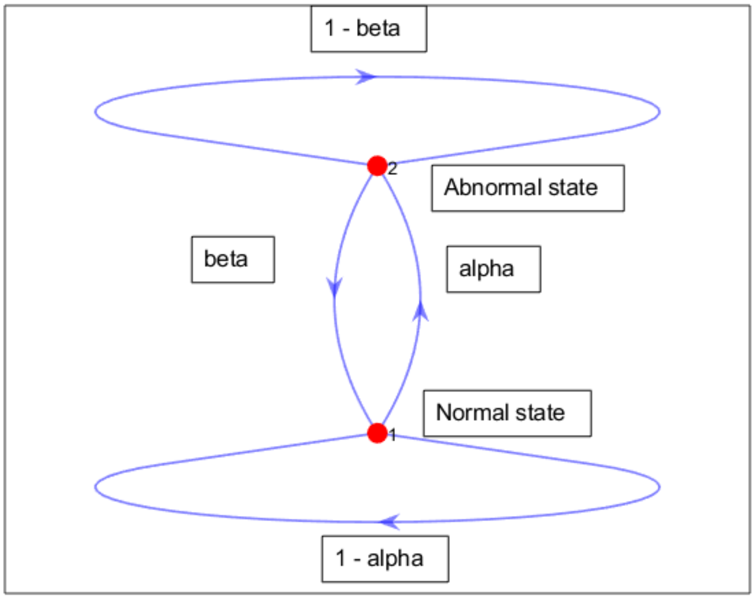

Figure 5.3: Markov's chain based event modeling.

5.3 Simulation Parameters and Assumptions

The simulator considers a network setup described above in the simulation description section. It considers a network with 6 sectors and 9 sensors in each sector. In a sector, three sensor nodes placed at the circumference of each concentric circles namely Z1, Z2, and Z3. The probability of state transition from state 1 to state 2 is alpha and is fixed as 0.01 for a few sectors and other sectors have increasing probability from 0.01 to 0.1. Based on the number of sectors with increasing alpha value, six network scenarios are defined. The probability of state transition from state 2 to state 1 is beta. There are three cases in each network scenario with beta values 0.1, 0.05, and 0.01. The simulator assumes that the sensor nodes transmit information periodically, with a period depending on their distance from energy transmitters, and the energy transmitter combination being used to energize them as described above. Figure 5.2 illustrate the sensor processing time and transmission interval information.

Also, it is assumed that the energy transmitter rotation time is very small as compared to the energy harvesting time and hence for simulation purposes, it is assumed to be zero.

5.4 Simulation Results

This section presents the detailed observations of the three schemes that are single Omnidirectional transmitter (scheme-1), one Omnidirectional in combination with sequential rotation of directional transmitter (scheme-2), and one Omnidirectional transmitter in combination with maximum alarm based rotation of the directional transmitter (scheme-3).

These schemes are simulated for 6 different network scenarios that are defined based on sector-wise increasing probability of the alarm generation (occurrence of abnormal events). Scenario-1 considers 1 active sector i.e. one sector has higher alarm generation rate compared to other sectors. For performance evaluations, we represent the alarm generation rate of the active sector by alpha and others are assumed to be the same (0.01). scenario-2 considers two active sectors with higher alarm generation rate alpha and the others set to (0.01). Scenarios 3, 4, 5 and 6 are defined similarly.

The performance of these schemes in different scenarios is evaluated in terms of

(a) The number of abnormal events detected.

(b) The number of alarm signals received per abnormal event.

5.4.1 Performance with Increasing Alarm Generation Ratio in the Active Sector

This section presents the performance variation when only one sector has alarms (scenario-1) with increasing alarm generation rate (alpha) and all other sectors have fixed and low alarm generation rate (0.01). The duration of alarm condition that is defined by probability that an event stays in the abnormal state (beta) is fixed at 0.1.

Figures 5.4 and 5.5 illustrate total abnormal events detected and alarms received in different schemes for scenario-1 with increasing alarm generation and beta = 0.1.

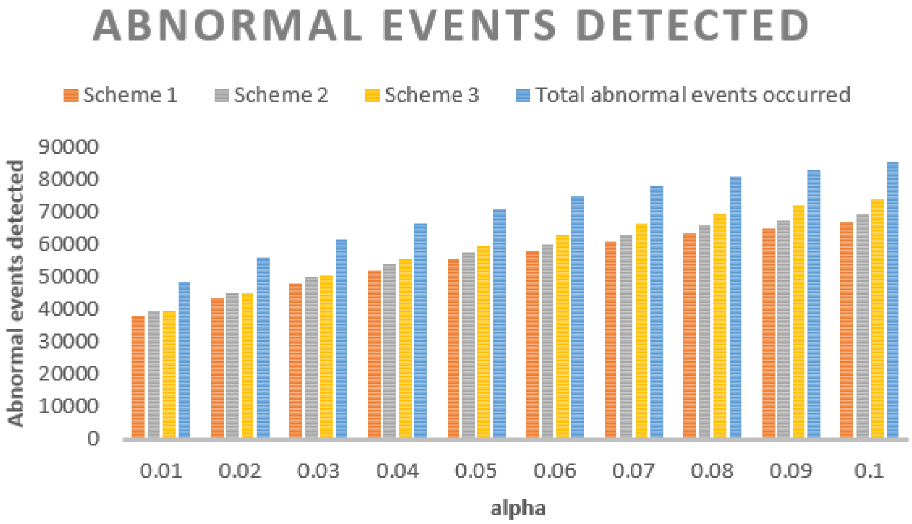

Figure 5.4: Total abnormal events detected for scenario-1 with increasing alarm generation rate.

As the alarm generation rate is increased, the abnormal events detected in different schemes also increases but, scheme-3 detects more number of abnormal events as compared to scheme-1 and scheme-2. This difference in detecting abnormal events, is significant for higher alarm generation rates. For an alarm generation rate of 0.1, scheme-3 detects 86.51% of abnormal events compared to 80.94% in scheme-2 and 78.21% in scheme-1.

In terms of number of alarms received per abnormal event, scheme-3 performs better than scheme-2 and scheme-1. For higher values of alarm generation rate, the alarms received per abnormal event is significantly higher in scheme-3 as compared to scheme-2 and scheme-1.

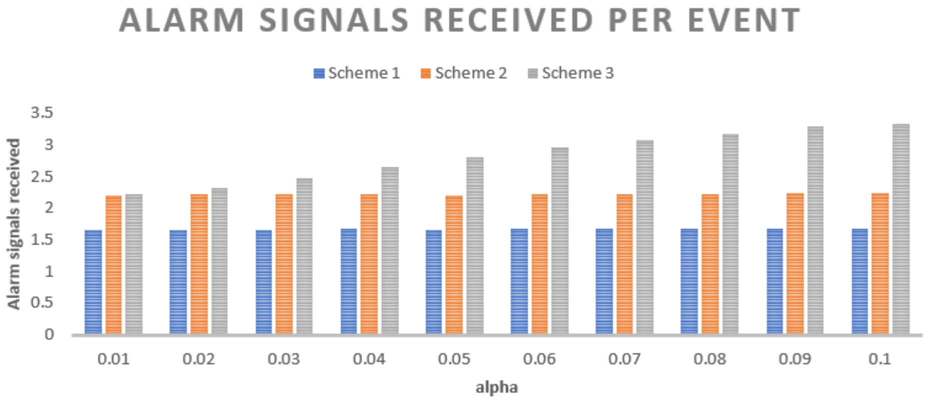

Figure 5.5: Total alarms received for scenario-1 increasing alarm generation rate.

5.4.2 Performance with Increasing Alarm State Duration

This section presents the performance variations with increasing duration of alarm condition (beta), when only one sector has alarms (scenario-1) with a higher alarm generation rate (alpha = 0.1) and all other sectors have fixed and low alarm generation rate (0.01). Figures 5.6 and 5.7 demonstrate the observations for scenario-1 with with increasing duration of alarm condition.

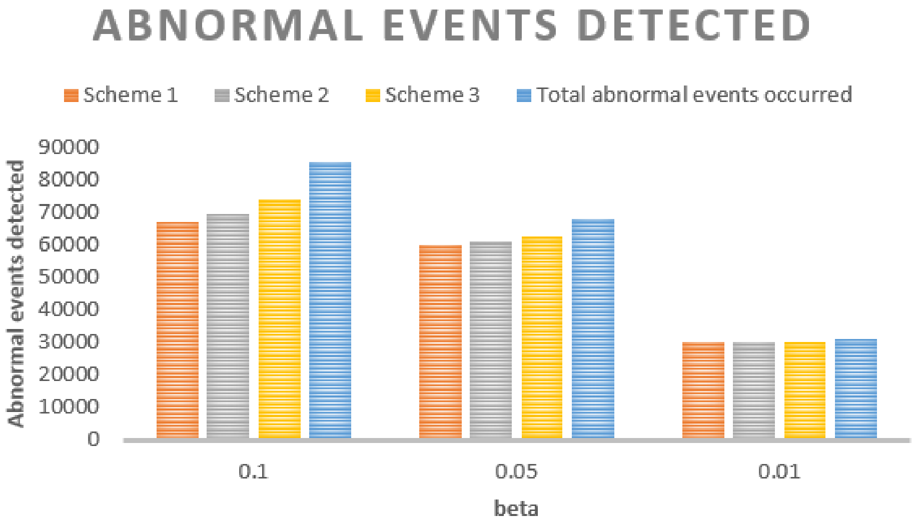

Figure 5.6: Total abnormal events detected for scenario 1 with increasing duration of alarm condition.

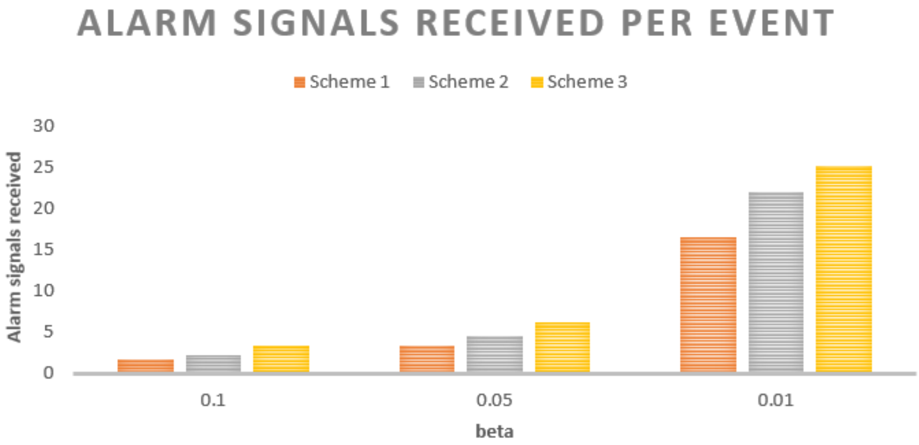

Figure 5.7: Total alarms received for scenario 1 with increasing duration of alarm condition.

As the duration of the alarm condition increases,the total number of abnormal events decrease. For shorter duration alarm condition, scheme-3 detects significantly higher percentage of abnormal events as compared to scheme-2 and scheme-1. With increasing duration of alarm condition, the performance in terms of detecting abnormal event for different schemes comes closer. Also, the total alarms received per abnormal event increases as the duration of the alarm condition increases.

5.4.3 Performance with Increasing Number of Active Sectors

This section presents the performance variation with increasing number of active sectors (scenario-1 to scenario-6) with a fixed alarm generation rate (alpha = 0.1) and duration of alarm condition that is defined by probability that an event stays in the abnormal state is fixed at beta = 0.05. Figures 5.8 and 5.9 illustrate the total abnormal events detected and total alarms received in different schemes for different scenarios with alpha = 0.1 and beta = 0.05.

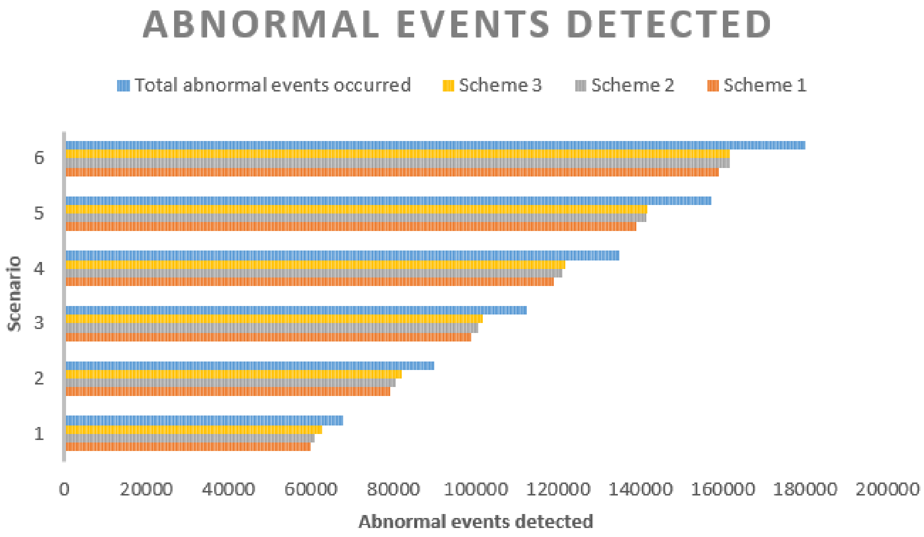

Figure 5.8: Total abnormal events detected in different schemes for different scenarios.

For lower number of active sectors, the abnormal event detection in scheme-3 is significantly higher as compared to scheme-1 and scheme-2. As the number of active sectors increase, the difference in abnormal event detection in different schemes comes closer but, scheme-3 performs better than scheme-1 and scheme-2 for all the cases. Similarly, in terms of alarms received per event, scheme-3 performs is significantly better as compared to scheme-1 and scheme-2 for lower number of active sectors. As the number of active sectors increase, the number of alarms received in scheme-3 and scheme-2 decrease in general but, scheme-3 performs better. The number of alarms received in scheme-1 does not change with increasing active sectors.

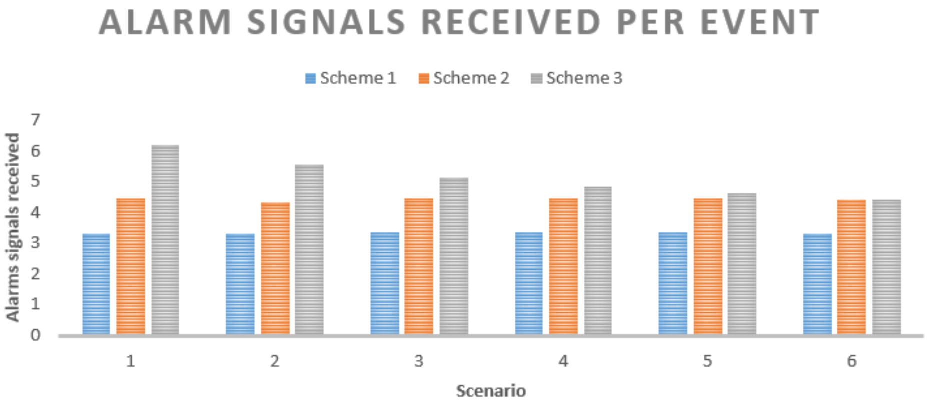

Figure 5.9: Total alarms received in different schemes for different scenarios.

CHAPTER 6: CONCLUSIONS AND FUTURE WORK

The performance of the deployment schemes can be analyzed based on the total abnormal events detected as compared to total abnormal event occurred in the network, and the total number of alarms received with respect to the total number of abnormal events occurred in the network. Beta value corresponds to the duration of an abnormal event. Smaller beta value indicates the events with longer duration. Alpha value corresponds to the total number of abnormal events. Larger alpha value indicates higher number of events for a specific beta value. As we decrease the beta value for a scenario, the total number of abnormal events decrease but the total number of alarms generated increase. This indicates that for a system with longer duration of abnormal events, there are more alarms generated with respect to an abnormal event.

For different network scenarios the following observations are made. Maximum flag based transmitter rotation scheme performs better than sequential transmitter rotation scheme in most of the network scenarios. As the number of active sectors is increased to six, the performance of both the schemes become similar. As compared to a single omnidirectional transmitter deployment (scheme 1), the combination of an omnidirectional transmitter and a directional (scheme 2 and scheme 3) performs significantly good in terms of both , total abnormal events detected and total number of alarms received per abnormal event occurred. The maximum alarm based transmitter rotation scheme achieves up to 98.06% of abnormal event detection in a network scenario where only one sector is active. In conclusion, maximum alarm based directional transmitter rotation scheme not only detects higher percentage of the abnormal event occurred in the network but also receives more alarms per abnormal event.

6.1 Additional Discussions and Future Scope

The physical rotation of directional antenna to increase the information reception is a proof of concept. The work presents a potential benefit of using a combination of omnidirectional antenna for getting periodic information from network and then beam steering to assist higher sampling rates from a concerned area. The above conclusion are based on the assumptions that were considered for the simulation. Hence, additional considerations and optimization is needed for the practical deployment for the scheme. Instead of directing beam to a area by physically rotating the antenna or energy transmitter, beam steering antenna could be considered for changing the direction of the main lobe of the radiation pattern by switching the antenna elements or by changing the phases of RF signal driving the elements.

For simulation purpose, the time of rotation is not considered for both sequential rotation and maximum alarm based rotation, but the practical system will take some time to direct the beam to a particular area. The scheme could be simulated with simple sensor node deployment and adding the time of rotation in it. Additionally, the relative energy harvesting time with omnidirectional and directional energy transmitters are chosen arbitrarily for simulation. The assumption is that with a combination of an omnidirectional and a directional energy transmitter, the sensor nodes take three times less time to harvest energy as compared to the time taken with only omnidirectional transmitter (with same total radiated RF power). However, the relative energy harvesting time could be better estimated by considering same total RF power with and without directional antenna and then determining optimum distribution of radiated power for omnidirectional and directional antennas.

In this work,the energy transmitters are placed at a fixed location covering a certain area. This can be combined with [30], where the transmitters are moved to different locations to provide energy to the sensor node. The combination of both the schemes could be used cover a large geographical area and, collect and maximize information from different locations. Also, it was observed that the total abnormal event captured and total alarms generated per abnormal event occurred is a function of the abnormal event duration and the sensor node placement (distance between sensor node and energy transmitter). If the average abnormal event duration is such that the most distant node can give at least one update within that duration, all the abnormal events can be captured. Hence if, the physical entity that we want to sense, is modeled in such a way that we could estimate the average duration of abnormal event, and the sensor nodes are deployed in such a way that the most distant node provides at least one update in that duration, all the abnormal events could be captured.

At present, the harvester board has capacitors with maximum value of 50 mF. A higher value capacitor could be used to prolong the sensor operation for different applications. Although a higher value capacitor will take more time to charge, there could be multiple transmission in a single harvesting cycle. The above transmitter and sensor deployment scheme and application based selection of capacitor value, could be used to design a feasible monitoring system for applications such as space exploration, environmental and industrial monitoring systems, etc.

REFERENCES

[1] S. Kim, R. Vyas, J. Bito, K. Niotaki, A. Collado, A. Georgiadis, and M. M. Tentzeris, “Ambient rf energy-harvesting technologies for self-sustainable standalone wireless sensor platforms,” *Proceedings of the IEEE*, vol. 102, no. 11, pp. 1649–1666, 2014.

[2] P. Kamalinejad, C. Mahapatra, Z. Sheng, S. Mirabbasi, V. C. M. Leung, and Y. L. Guan, “Wireless energy harvesting for the internet of things,” *IEEE Communications Magazine*, vol. 53, no. 6, pp. 102–108, 2015.

[3] K. Romer and F. Mattern, “The design space of wireless sensor networks,” *IEEE Wireless Communications*, vol. 11, no. 6, pp. 54–61, 2004.

[4] F. K. Shaikh and S. Zeadally, “Energy harvesting in wireless sensor networks: A comprehensive review,” *Renewable and Sustainable Energy Reviews*, vol. 55, pp. 1041 – 1054, 2016.

[5] K. Adu-Manu, N. Adam, C. Tapparello, H. Ayatollahi, and W. Heinzelman, “Energy-harvesting wireless sensor networks (eh-wsns): A review,” *ACM Transactions on Sensor Networks*, vol. 14, pp. 1–50, 04 2018.

[6] S. Sudevalayam and P. Kulkarni, “Energy harvesting sensor nodes: Survey and implications,” *IEEE Communications Surveys Tutorials*, vol. 13, no. 3, pp. 443–461, 2011.

[7] M. M. I. Rajib, *Design Considerations for Intermittently Connected Energy Harvesting Wireless Sensor Networks.* PhD thesis, The University of North Carolina at Charlotte, 2018.

[8] M. Sansoy, A. S. Buttar, and R. Goyal, “Empowering wireless sensor networks with rf energy harvesting,” in *2020 7th International Conference on Signal Processing and Integrated Networks (SPIN)*, pp. 273–277, 2020.

[9] T. Beng Lim, N. M. Lee, and B. K. Poh, “Feasibility study on ambient rf energy harvesting for wireless sensor network,” in *2013 IEEE MTT-S International Microwave Workshop Series on RF and Wireless Technologies for Biomedical and Healthcare Applications (IMWS-BIO)*, pp. 1–3, 2013.

[10] G. Verma and V. Sharma, “A survey on hardware design issues in rf energy harvesting for wireless sensor networks (wsn),” in *2016 5th International Conference on Wireless Networks and Embedded Systems (WECON)*, pp. 1–9, 2016.

[11] H. Nishimoto, Y. Kawahara, and T. Asami, “Prototype implementation of ambient rf energy harvesting wireless sensor networks,” in *SENSORS, 2010 IEEE*, pp. 1282–1287, 2010.

[12] X. Yang, C. Jiang, A. Z. Elsherbeni, F. Yang, and Y. Wang, "A novel compact printed rectenna for data communication systems," *IEEE Transactions on Antennas and Propagation*, vol. 61, no. 5, pp. 2532–2539, 2013.

[13] G. Monti, L. Corchia, and L. Tarricone, "Uhf wearable rectenna on textile materials," *IEEE Transactions on Antennas and Propagation*, vol. 61, no. 7, pp. 3869–3873, 2013.

[14] U. Olgun, C. Chen, and J. L. Volakis, "Investigation of rectenna array configurations for enhanced rf power harvesting," *IEEE Antennas and Wireless Propagation Letters*, vol. 10, pp. 262–265, 2011.

[15] P. Nintanavongsa, U. Muncuk, D. R. Lewis, and K. R. Chowdhury, "Design optimization and implementation for rf energy harvesting circuits," *IEEE Journal on Emerging and Selected Topics in Circuits and Systems*, vol. 2, no. 1, pp. 24–33, 2012.

[16] Z. PopoviÄ, S. Korhummel, S. Dunbar, R. Scheeler, A. Dolgov, R. Zane, E. Falkenstein, and J. Hagerty, "Scalable rf energy harvesting," *IEEE Transactions on Microwave Theory and Techniques*, vol. 62, no. 4, pp. 1046–1056, 2014.

[17] R. Zhang and C. K. Ho, "Mimo broadcasting for simultaneous wireless information and power transfer," *IEEE Transactions on Wireless Communications*, vol. 12, no. 5, pp. 1989–2001, 2013.

[18] I. Krikidis, "Simultaneous information and energy transfer in large-scale networks with/without relaying," *IEEE Transactions on Communications*, vol. 62, no. 3, pp. 900–912, 2014.

[19] G. Silver, C. I. Kolitsidas, O. BjÃ¶rkqvist, M. Matsson, O. Dahlberg, and B. L. G. Jonsson, "Exploiting antenna array configurations for efficient simultaneous wireless information and power transfer," in *2017 IEEE International Symposium on Antennas and Propagation USNC/URSI National Radio Science Meeting*, pp. 1083–1084, 2017.

[20] L. Liu, R. Zhang, and K. Chua, "Wireless information transfer with opportunistic energy harvesting," in *2012 IEEE International Symposium on Information Theory Proceedings*, pp. 950–954, 2012.

[21] B. Han, R. Nielsen, C. Papadias, and R. Prasad, "Radio frequency energy harvesting for long lifetime wireless sensor networks," in *2013 16th International Symposium on Wireless Personal Multimedia Communications (WPMC)*, pp. 1–5, 2013.

[22] G. Yang, C. K. Ho, and Y. L. Guan, "Dynamic resource allocation for multiple-antenna wireless power transfer," *IEEE Transactions on Signal Processing*, vol. 62, no. 14, pp. 3565–3577, 2014.

[23] D. Mishra, S. De, S. Jana, S. Basagni, K. Chowdhury, and W. Heinzelman, "Smart rf energy harvesting communications: challenges and opportunities," *IEEE Communications Magazine*, vol. 53, no. 4, pp. 70–78, 2015.

[24] C. Sergiou, V. Vassiliou, and K. Christou, "Rf energy harvesting in wireless sensor networks for critical aircraft systems â an experimental approach," in *2016 IEEE International Conference on Wireless for Space and Extreme Environments (WiSEE)*, pp. 178–183, 2016.

[25] A. Tripathi and A. Nasipuri, "Information based smart rf energy harvesting in wireless sensor networks," in *2019 IEEE 16th International Conference on Smart Cities: Improving Quality of Life Using ICT IoT and AI (HONET-ICT)*, pp. 197–198, 2019.

[26] A. Litvinenko, S. Tjukovs, D. Pikulins, and A. Aboltins, "The impact of waveform on the efficiency of wireless power transfer using prefabricated energy harvesting device," in *2018 International Conference on Information and Telecommunication Technologies and Radio Electronics (UkrMiCo)*, pp. 1–5, 2018.

[27] C. Kyprianou, C. Psomas, and I. Krikidis, "A green wireless powered sensor network: An experimental approach," in *2016 18th Mediterranean Electrotechnical Conference (MELECON)*, pp. 1–6, 2016.

[28] H. Choi, "Application for outdoor dust monitoring using rf wireless power transmission," in *2018 10th International Conference on Knowledge and Smart Technology (KST)*, pp. 196–199, 2018.

[29] M. A. Rosli, A. Ali, and N. Z. Yahaya, "Development of rf energy harvesting technique for li-fi application," in *2016 6th International Conference on Intelligent and Advanced Systems (ICIAS)*, pp. 1–6, 2016.

[30] F. Sangare, Y. Xiao, D. Niyato, and Z. Han, "Mobile charging in wireless-powered sensor networks: Optimal scheduling and experimental implementation," *IEEE Transactions on Vehicular Technology*, vol. 66, no. 8, pp. 7400–7410, 2017.

[31] https://www.powercastco.com/documentation/.

APPENDIX : MATLAB CODE

```

% RF energy harvesting WSN simulation.%
% Author: Asheesh Tripathi

clear;
clc;
sector = struct([]);
num_of_sectors = 6;   %total number of sectors.
num_of_sensors = 9;  %total number of sensors in a sector.
% Flag generation based on probabilities of state transition.
     for each sector id (1 to 6) and
% corresponding sensor id(1 to 9), we independently generate
    total 100000 flags each. total flag
% is total numbers of flag with value 1 in each sector.

for secID = 1 : num_of_sectors
     if(  secID == 3  )
         p_00 = 0.90;               % probability of state
             transition 1-alpha.
         p_01 = 1 - p_00;           % probability of state
             transition alpha.
         p_10 = 0.01;               % probability of state
             transition beta.
         p_11 = 1 - p_10;           % probability of state
             transition 1-beta.
     else
         p_00 = 0.99;             % probability of state
             transition 1-alpha.
         p_01 = 1 - p_00;         % probability of state
             transition alpha.
         p_10 = 0.01;             % probability of state
             transition beta.
         p_11 = 1 - p_10;         % probability of state
             transition 1-beta.
     end
     tmp = 0;
     for sensID = 1 : num_of_sensors
          P = [p_00 p_01; p_10 p_11];
          mc = dtmc(P);
          X = simulate(mc,100008);
             for i = 1:100008
              if(X(i) == 1)
                  sector(secID).sensor(sensID).flag(i) = 0;
              else
                   sector(secID).sensor(sensID).flag(i) = 1;
              end
             end
          total_sensor_flag(sensID) = nnz(sector(secID).sensor(
              sensID).flag);
          for j=1:24:100000
               if(sensID == 1|2|3)
          sector(secID).sensor(sensID).flag_up(j) = sector(
              secID).sensor(sensID).flag(j);
          sector(secID).sensor(sensID).flag_up(j+1:j+5) = [0 0
              0 0 0];
          sector(secID).sensor(sensID).flag_up(j+6) = sector(
              secID).sensor(sensID).flag(j+6);
          sector(secID).sensor(sensID).flag_up(j+7:j+11) = [0 0
               0 0 0];
          sector(secID).sensor(sensID).flag_up(j+12) = sector(
              secID).sensor(sensID).flag(j+12);
          sector(secID).sensor(sensID).flag_up(j+13:j+17) = [0
              0 0 0 0];
          sector(secID).sensor(sensID).flag_up(j+18) = sector(
              secID).sensor(sensID).flag(j+18);
          sector(secID).sensor(sensID).flag_up(j+19:j+23) = [0
              0 0 0 0];
              elseif(sensID == 5|6|7)
          sector(secID).sensor(sensID).flag_up(j)    = sector(
              secID).sensor(sensID).flag(j);
          sector(secID).sensor(sensID).flag_up(j+1:j+11) = [0 0
               0 0 0 0 0 0 0 0 0];
          sector(secID).sensor(sensID).flag_up(j+12) = sector(
              secID).sensor(sensID).flag(j+12);
          sector(secID).sensor(sensID).flag_up(j+13:j+23) = [0
              0 0 0 0 0 0 0 0 0 0];
               else
          sector(secID).sensor(sensID).flag_up(j) = sector(
              secID).sensor(sensID).flag(j);
          sector(secID).sensor(sensID).flag_up(j+1:j+23) = [0 0 0 0 0 0 0 0 0 0 0 0 0 0 0 0 0 0 0 0 0 0 0];
              end
          end
          total_sensor_flag_up(sensID) = nnz(sector(secID).sensor(sensID).flag_up);
      end
      total_flag(secID) = sum(total_sensor_flag);
       total_flag_up(secID) = sum(total_sensor_flag_up);
end

% periodic and intermediate update in 1 omnidirectional and 1 directional
% transmitter scenario. Directional transmitter provide energy to each
% sector in sequential manner for intermediate updates.

sec = 1;
for k = 1:24:100000
    for secID = 1: num_of_sectors
      for sensID = 1 : num_of_sensors
          if(sensID == 1|2|3)
        sector(secID).sensor(sensID).flag_update_2(k)   = sector(secID).sensor(sensID).flag(k);
        sector(secID).sensor(sensID).flag_update_2(k+1:k+5) = [0 0 0 0 0];
        sector(secID).sensor(sensID).flag_update_2(k+6) =
              sector(secID).sensor(sensID).flag(k+6);
          sector(secID).sensor(sensID).flag_update_2(k+7:k+11)
              = [0  0  0  0  0];
          sector(secID).sensor(sensID).flag_update_2(k+12) =
              sector(secID).sensor(sensID).flag(k+12);
          sector(secID).sensor(sensID).flag_update_2(k+13:k+17)
               = [0  0  0  0  0];
          sector(secID).sensor(sensID).flag_update_2(k+18) =
              sector(secID).sensor(sensID).flag(k+18);
          sector(secID).sensor(sensID).flag_update_2(k+19:k+23)
               = [0  0  0  0  0];
          sector(sec).sensor(sensID).flag_update_2(k)     =
              sector(sec).sensor(sensID).flag(k);
          sector(sec).sensor(sensID).flag_update_2(k+1)    = 0;
          sector(sec).sensor(sensID).flag_update_2(k+2)    =
              sector(sec).sensor(sensID).flag(k+2);
          sector(sec).sensor(sensID).flag_update_2(k+3)    = 0;
          sector(sec).sensor(sensID).flag_update_2(k+4)    =
              sector(sec).sensor(sensID).flag(k+4);
          sector(sec).sensor(sensID).flag_update_2(k+5)    = 0;
          sector(sec).sensor(sensID).flag_update_2(k+6)    =
              sector(sec).sensor(sensID).flag(k+6);
          sector(sec).sensor(sensID).flag_update_2(k+7)    = 0;
          sector(sec).sensor(sensID).flag_update_2(k+8)    =
              sector(sec).sensor(sensID).flag(k+8);
          sector(sec).sensor(sensID).flag_update_2(k+9)    = 0;
          sector(sec).sensor(sensID).flag_update_2(k+10)    =
              sector(sec).sensor(sensID).flag(k+10);
          sector(sec).sensor(sensID).flag_update_2(k+11)    = 0;
          sector(sec).sensor(sensID).flag_update_2(k+12)    =
              sector(sec).sensor(sensID).flag(k+12);
          sector(sec).sensor(sensID).flag_update_2(k+13)    = 0;
          sector(sec).sensor(sensID).flag_update_2(k+14)    =
              sector(sec).sensor(sensID).flag(k+14);
          sector(sec).sensor(sensID).flag_update_2(k+15)    = 0;
          sector(sec).sensor(sensID).flag_update_2(k+16)    =
              sector(sec).sensor(sensID).flag(k+16);
          sector(sec).sensor(sensID).flag_update_2(k+17)    = 0;
          sector(sec).sensor(sensID).flag_update_2(k+18)    =
              sector(sec).sensor(sensID).flag(k+18);
          sector(sec).sensor(sensID).flag_update_2(k+19)    = 0;
          sector(sec).sensor(sensID).flag_update_2(k+20)    =
              sector(sec).sensor(sensID).flag(k+20);
          sector(sec).sensor(sensID).flag_update_2(k+21)    = 0;
          sector(sec).sensor(sensID).flag_update_2(k+22)    =
              sector(sec).sensor(sensID).flag(k+22);
          sector(sec).sensor(sensID).flag_update_2(k+23)    = 0;
            elseif(sensID == 5|6|7)
          sector(secID).sensor(sensID).flag_update_2(k) =
              sector(secID).sensor(sensID).flag(k);
          sector(secID).sensor(sensID).flag_update_2(k+1:k+11)
              = [0 0 0 0 0 0 0 0 0 0 0];
          sector(secID).sensor(sensID).flag_update_2(k+12) =
              sector(secID).sensor(sensID).flag(k);
          sector(secID).sensor(sensID).flag_update_2(k+13:k+23) = [0 0 0 0 0 0 0 0 0 0 0];
          sector(sec).sensor(sensID).flag_update_2(k) = sector(sec).sensor(sensID).flag(k);
              sector(sec).sensor(sensID).flag_update_2(k+1:k+3) = [0 0 0];
          sector(sec).sensor(sensID).flag_update_2(k+4) = sector(sec).sensor(sensID).flag(k+4);
          sector(sec).sensor(sensID).flag_update_2(k+5:k+7) = [0 0 0];
              sector(sec).sensor(sensID).flag_update_2(k+8) = sector(sec).sensor(sensID).flag(k+8);
          sector(sec).sensor(sensID).flag_update_2(k+9:k+11) = [0 0 0];
          sector(sec).sensor(sensID).flag_update_2(k+12) = sector(sec).sensor(sensID).flag(k+12);
              sector(sec).sensor(sensID).flag_update_2(k+13:k+15) = [0 0 0];
          sector(sec).sensor(sensID).flag_update_2(k+16) = sector(sec).sensor(sensID).flag(k+16);
          sector(sec).sensor(sensID).flag_update_2(k+17:k+19) = [0 0 0];
              sector(sec).sensor(sensID).flag_update_2(k+20) = sector(sec).sensor(sensID).flag(k+20);
          sector(sec).sensor(sensID).flag_update_2(k+21:k+23) = [0 0 0];
            else
```

```
        sector(secID).sensor(sensID).flag_update_2(k) = sector(secID).sensor(sensID).flag(k);
        sector(secID).sensor(sensID).flag_update_2(k+1:k+23) = [0 0 0 0 0 0 0 0 0 0 0 0 0 0 0 0 0 0 0 0 0 0 0];
        sector(sec).sensor(sensID).flag_update_2(k) = sector(sec).sensor(sensID).flag(k);
        sector(sec).sensor(sensID).flag_update_2(k+1:k+7) = [0 0 0 0 0 0 0];
        sector(sec).sensor(sensID).flag_update_2(k+8) = sector(sec).sensor(sensID).flag(k+8);
        sector(sec).sensor(sensID).flag_update_2(k+9:k+15) = [0 0 0 0 0 0 0];
        sector(sec).sensor(sensID).flag_update_2(k+16) = sector(sec).sensor(sensID).flag(k+16);
        sector(sec).sensor(sensID).flag_update_2(k+17:k+23) = [0 0 0 0 0 0 0];
          end

        total_sensor_flag_update_2(sensID) = nnz(sector(secID).sensor(sensID).flag_update_2);
      end
        total_flag_update_2(secID) = sum(total_sensor_flag_update_2);
    end
     sec = sec + 1;
     if(sec > 6)
     sec = 1;
     end
end

% periodic and intermediate update in 1 omnidirectional and 1 directional
% transmitter scenario. Directional transmitter provide energy to a
% sector with maximum flags counted at every periodic update.

sec_1 = 1;
pr_sec_1 = 0;
for m = 1:24:100000
    for secID = 1: num_of_sectors
      for sensID = 1 : num_of_sensors
              if(sensID == 1|2|3)
        sector(secID).sensor(sensID).flag_update_3(m) = sector(secID).sensor(sensID).flag(m);
        sector(secID).sensor(sensID).flag_update_3(m+1:m+5) = [0 0 0 0 0];
        sector(secID).sensor(sensID).flag_update_3(m+6) = sector(secID).sensor(sensID).flag(m+6);
        sector(secID).sensor(sensID).flag_update_3(m+7:m+11) = [0 0 0 0 0];
        sector(secID).sensor(sensID).flag_update_3(m+12) = sector(secID).sensor(sensID).flag(m+12);
        sector(secID).sensor(sensID).flag_update_3(m+13:m+17) = [0 0 0 0 0];
```

```
            sector(secID).sensor(sensID).flag_update_3(m+18) = sector(secID).sensor(sensID).flag(m+18);
            sector(secID).sensor(sensID).flag_update_3(m+19:m+23) = [0 0 0 0 0];
            sector(sec_1).sensor(sensID).flag_update_3(m) = sector(sec_1).sensor(sensID).flag(m);
            sector(sec_1).sensor(sensID).flag_update_3(m+1) = 0;
            sector(sec_1).sensor(sensID).flag_update_3(m+2) = sector(sec_1).sensor(sensID).flag(m+2);
            sector(sec_1).sensor(sensID).flag_update_3(m+3) = 0;
            sector(sec_1).sensor(sensID).flag_update_3(m+4) = sector(sec_1).sensor(sensID).flag(m+4);
            sector(sec_1).sensor(sensID).flag_update_3(m+5) = 0;
            sector(sec_1).sensor(sensID).flag_update_3(m+6) = sector(sec_1).sensor(sensID).flag(m+6);
            sector(sec_1).sensor(sensID).flag_update_3(m+7) = 0;
            sector(sec_1).sensor(sensID).flag_update_3(m+8) = sector(sec_1).sensor(sensID).flag(m+8);
            sector(sec_1).sensor(sensID).flag_update_3(m+9) = 0;
            sector(sec_1).sensor(sensID).flag_update_3(m+10) = sector(sec_1).sensor(sensID).flag(m+10);
            sector(sec_1).sensor(sensID).flag_update_3(m+11) = 0;
            sector(sec_1).sensor(sensID).flag_update_3(m+12) = sector(sec_1).sensor(sensID).flag(m+12);
            sector(sec_1).sensor(sensID).flag_update_3(m+13) = 0;
            sector(sec_1).sensor(sensID).flag_update_3(m+14) = sector(sec_1).sensor(sensID).flag(m+14);
            sector(sec_1).sensor(sensID).flag_update_3(m+15) = 0;
            sector(sec_1).sensor(sensID).flag_update_3(m+16) =
               sector(sec_1).sensor(sensID).flag(m+16);
            sector(sec_1).sensor(sensID).flag_update_3(m+17) = 0;
            sector(sec_1).sensor(sensID).flag_update_3(m+18) =
               sector(sec_1).sensor(sensID).flag(m+18);
            sector(sec_1).sensor(sensID).flag_update_3(m+19) = 0;
            sector(sec_1).sensor(sensID).flag_update_3(m+20) =
               sector(sec_1).sensor(sensID).flag(m+20);
            sector(sec_1).sensor(sensID).flag_update_3(m+21) = 0;
            sector(sec_1).sensor(sensID).flag_update_3(m+22) =
               sector(sec_1).sensor(sensID).flag(m+22);
            sector(sec_1).sensor(sensID).flag_update_3(m+23) = 0;
                elseif(sensID == 4|5|6)
            sector(secID).sensor(sensID).flag_update_3(m) =
               sector(secID).sensor(sensID).flag(m);
            sector(secID).sensor(sensID).flag_update_3(m+1:m+11)
              = [0 0 0 0 0 0 0 0 0 0 0];
            sector(secID).sensor(sensID).flag_update_3(m+12) =
               sector(secID).sensor(sensID).flag(m+6);
            sector(secID).sensor(sensID).flag_update_3(m+13:m+23)
               = [0 0 0 0 0 0 0 0 0 0 0];
            sector(sec_1).sensor(sensID).flag_update_3(m) =
               sector(sec_1).sensor(sensID).flag(m);
            sector(sec_1).sensor(sensID).flag_update_3(m+1:m+3) =
               [0 0 0];
            sector(sec_1).sensor(sensID).flag_update_3(m+4) =
    sector(sec_1).sensor(sensID).flag(m+4);
        sector(sec_1).sensor(sensID).flag_update_3(m+5:m+7) = [0 0 0];
        sector(sec_1).sensor(sensID).flag_update_3(m+8) = sector(sec_1).sensor(sensID).flag(m+8);
        sector(sec_1).sensor(sensID).flag_update_3(m+9:m+11) = [0 0 0];
        sector(sec_1).sensor(sensID).flag_update_3(m+12) = sector(sec_1).sensor(sensID).flag(m+12);
        sector(sec_1).sensor(sensID).flag_update_3(m+13:m+15) = [0 0 0];
        sector(sec_1).sensor(sensID).flag_update_3(m+16) = sector(sec_1).sensor(sensID).flag(m+16);
        sector(sec_1).sensor(sensID).flag_update_3(m+17:m+19) = [0 0 0];
        sector(sec_1).sensor(sensID).flag_update_3(m+20) = sector(sec_1).sensor(sensID).flag(m+20);
        sector(sec_1).sensor(sensID).flag_update_3(m+21:m+23) = [0 0 0];

            else
        sector(secID).sensor(sensID).flag_update_3(m) = sector(secID).sensor(sensID).flag(m);
        sector(secID).sensor(sensID).flag_update_3(m+1:m+23) = [0 0 0 0 0 0 0 0 0 0 0 0 0 0 0 0 0 0 0 0 0 0 0];
        sector(sec_1).sensor(sensID).flag_update_3(m) = sector(sec_1).sensor(sensID).flag(m);
        sector(sec_1).sensor(sensID).flag_update_3(m+1:m+7) = [0 0 0 0 0 0 0];
        sector(sec_1).sensor(sensID).flag_update_3(m+8) = sector(sec_1).sensor(sensID).flag(m+8);
        sector(sec_1).sensor(sensID).flag_update_3(m+9:m+15) = [0 0 0 0 0 0 0];
        sector(sec_1).sensor(sensID).flag_update_3(m+16) = sector(sec_1).sensor(sensID).flag(m+16);
        sector(sec_1).sensor(sensID).flag_update_3(m+17:m+23) = [0 0 0 0 0 0 0];
              end
        total_sensor_flag_update_3(sensID) = nnz(sector(secID).sensor(sensID).flag_update_3);
        total_sensor_flag_1(sensID) = nnz(sector(secID).sensor(sensID).flag(m));

        total_flag_update_3(secID) = sum(total_sensor_flag_update_3);
        total_flag_1(secID) = sum(total_sensor_flag_1);
      end

    end
     [maxFlag, maxID] =  max([total_flag_1]);
     sec_1 = maxID;
end
total_fl = sum(total_flag);
total_up_1 = sum(total_flag_up);
```

```
total_up_2 = sum(total_flag_update_2);
total_up_3 = sum(total_flag_update_3);
% This section counts the total number of abnormal events occurred and
% total abnormal events captured in diffrent schemes.
 a=0;
 b=0;  count = 0;
 count_1 = 0;
 count_2 = 0;
 count_3 = 0;
 for secID = 1: num_of_sectors
      for sensID = 1 : num_of_sensors
        for z = 1:100000
            if(sector(secID).sensor(sensID).flag(z) == 1)
                if a == 0
                   a = z;
                end
                if z == 100000
                    b = z;
                    count = count + 1;
                    %cond check
                    if(nnz(sector(secID).sensor(sensID).flag_up(a:b)) >= 1)
                        count_1 = count_1 + 1;
                    end
                    if(nnz(sector(secID).sensor(sensID).flag_update_2(a:b)) >= 1)
                        count_2 = count_2 + 1;
                    end
                    if(nnz(sector(secID).sensor(sensID).flag_update_3(a:b)) >= 1)
                        count_3 = count_3 + 1;
                    end
                    a = 0;
                    b = 0;
                elseif(sector(secID).sensor(sensID).flag(z + 1) == 0)
                    b = z;
                    count = count + 1;
                    %cond check
                    if(nnz(sector(secID).sensor(sensID).flag_up(a:b)) >= 1)
                        count_1 = count_1 + 1;
                    end
                    if(nnz(sector(secID).sensor(sensID).flag_update_2(a:b)) >= 1)
                        count_2 = count_2 + 1;
                    end
                    if(nnz(sector(secID).sensor(sensID).flag_update_3(a:b)) >= 1)
                        count_3 = count_3 + 1;
                    end
                    a = 0;
                    b = 0;
```

```
               end
           end
       end
     end
end
```